POLITECNICO DI TORINO
Repository ISTITUZIONALE

Green façades and climate resilience: A comparative analysis across retrofit scenarios for an Italian building archetype in two representative climatic contexts

Original
Green façades and climate resilience: A comparative analysis across retrofit scenarios for an Italian building archetype in two representative climatic contexts / Pourabdollahtootkaboni, M., Ballarini, I., Corrado, V., Susca, T., Zanghirella, F.. - In: ENERGY AND BUILDINGS. - ISSN 0378-7788. - ELETTRONICO. - 373:(2026), pp. 1-16. [10.1016/j.enbuild.2026.118336]

Availability:
This version is available at: 11583/3016691 since: 2026-10-15T13:03:50Z

Publisher:
Elsevier

Published
DOI:10.1016/j.enbuild.2026.118336

Terms of use:

This article is made available under terms and conditions as specified in the corresponding bibliographic description in the repository

Publisher copyright

(Article begins on next page)

27 October 2026

Energy & Buildings 373 (2026) 118336

Contents lists available at ScienceDirect

Energy & Buildings

journal homepage: www.elsevier.com/locate/enb

Green façades and climate resilience: A comparative analysis across retrofit scenarios for an Italian building archetype in two representative climatic contexts☆

Mamak P. Tootkaboni [a,*], Ilaria Ballarini [a], Vincenzo Corrado [a], Tiziana Susca [b], Fabio Zanghirella [b]

[a] Department of Energy "Galileo Ferraris", Politecnico di Torino, Torino, Italy
[b] Italian National Agency for New Technologies, Energy and Sustainable Economic Development (ENEA), Rome, Italy

ARTICLE INFO

Keywords:
Green façades
Simulation of green façade
Climate change
Building energy performance
Ventilative cooling
Resilient cooling technologies

ABSTRACT

Accounting for 32% of global energy consumption, buildings not only impact climate change but are also affected by it. To address these challenges, in addition to decarbonising the building stock, there is a need to implement climate-resilient solutions that enhance climate adaptation. The proposed study explores the energy efficiency and climate resilience of non-traditional solutions like green façades for a representative Italian residential building archetype in two distinct climate zones, Rome and Turin, under current (2020s) and projected (2050s and 2090s) climate scenarios. The green façade is analysed using a detailed calculation tool implemented within the EnergyPlus (version 23.2) energy simulation software. The analysis covers both existing buildings without insulation and buildings retrofitted with insulation, solar shading, and ventilative cooling.

Results indicate that green façades—particularly when applied to multi-orientations of the building—can significantly reduce cooling need and overheating in pre-retrofit buildings, with reductions of up to 59% and 85%, respectively. In retrofitted buildings, green façades offer additional benefits beyond standard retrofit packages, with further cooling need reductions of up to 24.7% and decreasing overheating by up to 54.8%. Although their relative effectiveness generally declines with climate change due to rising temperatures and reduced plant evapotranspiration, green façades continue to provide relevant benefits even under the 2090s scenario. A comparison between the two climate zones reveals greater cooling reductions in Rome due to higher summer heat loads and lower winter heating penalties. These findings underscore the green façade potential as a passive design strategy to support the transition towards more sustainable and climate-resilient residential buildings.

1. Introduction

Climate change is one of the most critical global challenges, with profound implications for the built environment. In the European Union, the building sector accounts for approximately 40% of final energy consumption and 36% of energy-related greenhouse gas (GHG) emissions [1]. Consequently, buildings are both major contributors to climate change and among the most vulnerable systems to its impacts [2,3]. As global temperatures rise, the balance between heating and cooling demands is shifting in many regions, with growing concern over overheating risk and added stress on technical building systems, particularly cooling systems [4]. This issue is especially critical in urban areas, which currently accommodate the majority of the global population [5], act as significant GHG emitters [6], and serve as focal points for both global and local warming [7].

The urban heat island (UHI) effect—caused by the replacement of natural surfaces with artificial materials that store heat and inhibit evaporation—exacerbates urban temperatures compared to rural surroundings [8]. The consequences of elevated urban temperatures include increased rates of morbidity and mortality among urban populations [9,10], growing building cooling energy demand with

☆ This article is part of a Special issue entitled: 'NBS for Climate Change' published in Energy & Buildings.

* Corresponding author at: Department of Energy, Politecnico di Torino, corso Duca degli Abruzzi 24, 10129 Torino, Italy.
E-mail addresses: mamak.ptootkaboni@polito.it (M. P. Tootkaboni), ilaria.ballarini@polito.it (I. Ballarini), vincenzo.corrado@polito.it (V. Corrado), tiziana.susca@enea.it (T. Susca), fabio.zanghirella@enea.it (F. Zanghirella).

https://doi.org/10.1016/j.enbuild.2026.118336
Received 30 September 2025; Received in revised form 27 September 2026; Accepted 30 September 2026
Available online 1 October 2026
0378-7788/© 2026 The Authors. Published by Elsevier B.V. This is an open access article under the CC BY license (http://creativecommons.org/licenses/by/4.0/).

Nomenclature

Acronyms

DHT	Dynamic Heat Transfer
EBC	Energy in Buildings and Communities
EMS	Energy Management System
GF	Green Façade
GHG	Green House Gas
IEA	International Energy Agency
KPI	Key Performance Indicator
LAI	Leaf Area Index
RCP	Representative Concentration Pathway
REHVA	Federation of European Heating, Ventilation and Air Conditioning Associations
TMY	Typical Meteorological Year
UHI	Urban Heat Island
VC Tool	Ventilative Cooling Potential Tool
VPD	Vapour Pressure Deficit

Quantities

A	area (m^2)
ACH	air changes per hour (h^{-1})
EP	energy performance ($kWh \cdot m^{-2}$)
g	total solar energy transmittance (solar factor) (−)
HE	hours of exceedance (h)
K	areal heat capacity
q	(areic) heat flux ($W \cdot m^{-2}$)
U	thermal transmittance ($W \cdot m^{-2} K^{-1}$)
V	volume (m^3)
WHE	weighted hours of exceedance (h)
α	absorptance (−)
τ	transmittance (−)

Subscripts

add	additional
bare	bare wall
C	space cooling
cond	conduction
conv	convection
env	envelope
evap	evapotranspiration
g	gross
gl	glazing
H	space heating
lw	longwave radiation (infrared)
nd	need
sh	shading
sw	shortwave radiation (solar)
v	vegetation
w	wall

implications for energy security [11], deterioration of urban ecosystems [12], and declining air quality [13]. Huang et al. [10] reported that UHI-associated mortality is higher in cities in the southern and eastern parts of Europe, which are more exposed to high-temperature days. Additionally, a rise of just 1 °C in urban temperatures can increase electricity consumption and peak load by 0.5–8.5% and by approximately 21 (±10.4) W per person, respectively [14], potentially leading to blackouts and energy insecurity.

These climate- and urban-related conditions not only increase heat exposure but also reduce the efficacy of conventional energy retrofit strategies. While thermal insulation and airtightness are essential for reducing heating demand, highly insulated buildings may underperform or even worsen indoor thermal comfort during summer months if not complemented by passive and active cooling measures [15–17].

In response to these intensifying risks, the concept of resilient cooling has emerged as a crucial strategy to ensure that buildings remain thermally safe, comfortable, and functional under both typical conditions and during extreme climate events. These two dimensions are complementary. The first concerns long-term climate trends, such as changes in annual energy needs and indoor thermal comfort conditions over future time horizons. The second concerns short-duration extreme conditions, such as heatwave events. From a broader resilience perspective, these dimensions should be considered jointly, since a transition towards resilience depends on the capacity to respond to extreme events while also adapting to long-term trends and changing trajectories [18,19].

The IEA EBC Annex 80 – Resilient Cooling of Buildings – defines resilient cooling as "low-energy and low-emission cooling solutions that strengthen the ability of individuals and communities to withstand, recover, and adapt to climate-related heat stress" [20]. This paradigm marks a shift from an exclusive focus on energy efficiency to a broader emphasis on robustness and adaptability across different time scales and climate change-induced events. Annex 80 classifies solutions into passive, hybrid, and active categories, with a particular focus on passive and low-energy strategies—such as climate-responsive building elements, ventilation, shading, and vegetation—that limit reliance on mechanical cooling. In the review of resilient cooling strategies, four resilience capacities—absorptive, adaptive, restorative, and recovery—are increasingly recognized for their dual role in mitigating overheating and providing co-benefits. These co-benefits are essential for evaluating whether cooling systems can continue to function or quickly recover during disruptive events. Nature-based solutions, including green roofs and façades, are explicitly highlighted as part of passive strategies that reduce indoor overheating while delivering additional benefits for cities [21]. Similarly, the Guide of The Federation of European Heating, Ventilation and Air Conditioning Associations (REHVA) on Resilient Cooling underscores the role of vegetation-based measures, especially in buildings where access to active systems is limited [22].

Vegetation-based strategies offer significant potential for both building-level and urban-scale interventions. For instance, parks in Addis Ababa are shown to decrease air temperature by up to 6.72 °C, with cooling effects extending 240 m beyond the park boundaries [23]. In Manchester, a 5% increase in urban tree cover was associated with a 5% reduction in cooling energy [24]. In high-density urban areas with limited space for new green infrastructure, buildings offer valuable surfaces for vegetation integration, including green roofs and walls. These latter include both green façades and living walls. Green façades and living walls differ primarily in the position of the growing medium. In green façades, the substrate is placed horizontally on the ground or at different heights along the façade, whereas in living walls, the growing medium is positioned vertically, either directly attached to the façade or installed detached from it [25].

While green roofs can achieve substantial reductions in building energy use—up to 60% for heating and 70% for cooling in non-insulated buildings and up to 10% and 30%, respectively, when installed on insulated rooftops [26]—their impact on urban microclimates is limited when applied on high-rise structures [23,24]. In contrast, green walls can cover a remarkable share of urban vertical surfaces—up to twice the building footprint [28]—and contribute to both urban cooling and building energy efficiency, depending on multiple variables such as climate, urban geometry, façade orientation, plant coverage, and leaf area index (LAI) [29–32]. Iaria and Susca (2022) [26] demonstrated that, in the Mediterranean climate, the cooling effect of green façades and living walls at pedestrian level (i.e., at 2 m from the ground level) increases with the building height (up to ~20 m) and plant coverage,

with a near-linear relationship between coverage and temperature mitigation. LAI was found to be a key determinant of cooling potential for green façades. The UHI adaptation potential of green façades is almost negligible when LAI equals 1.5 and increases almost linearly with the increase in LAI. Besides, as far as living walls are concerned, LAI plays a more limited role since water evaporation is provided by the substrate layer. Nevertheless, for both green façades and living walls, the percentage of plant coverage and LAI are more influential in mitigating air temperatures than the building height [27]. The air mitigation potential of green walls also depends on the building arrangement. A study investigating the effect of green wall installation has shown that in Turin, green walls are more efficient in decreasing UHI when installed in street canyons parallel to the main wind direction [33]. In terms of energy performance, green walls have been shown to reduce heating and cooling demand by up to 16.5% and ~ 51%, respectively, particularly when applied across the whole building envelope [34].

Both green roofs and green walls can provide several environmental and societal co-benefits. Building-integrated vegetation technologies can contribute to noise attenuation [35,36], reduce air pollutants and sequester carbon [37–40], regulate stormwater runoff and improve water quality [41–44], enhance urban biodiversity [45,46], and contribute to urban beautification while providing aesthetic and psychological benefits [47–49].

Despite the well-documented benefits of building-integrated vegetation technologies, several barriers still hinder the widespread adoption of both green roofs and green walls. Knifka et al. [50] identified the lack of financial resources or willingness to bear installation costs, limited social acceptance and motivation, and challenges related to the practical and technical implementation of green façades as the most significant barriers to their deployment. Similarly, in the case of living walls, both installation and maintenance costs represent major limitations to their large-scale diffusion [51]. Ascione et al. [52] reviewed the literature on green wall systems, emphasizing, among other aspects, the technical relevance of the back wall. For direct green façades, the substrate wall should be free of holes and cracks to prevent the infiltration of climbing plants and the resulting risk of structural deterioration. Furthermore, in living wall systems, a crucial technical issue concerns the protection of the building envelope against water infiltration, which can be ensured either by installing a waterproof membrane or by providing an air gap between the living wall and the building envelope.

Regarding green roofs, additional technical constraints are associated with their applicability. Intensive and extensive green roofs are generally suitable for flat or moderately sloped rooftops to ensure adequate rainwater retention, whereas extensive green roofs cannot be used for recreational purposes because of their limited structural resistance [53]. In terms of public perception, green roofs are widely recognized as effective measures for mitigating urban overheating and improving building energy efficiency; however, the willingness to pay for their installation on private buildings remains limited. Conversely, public acceptance and willingness to invest in green roofs for public buildings are generally higher. This discrepancy is mainly related to concerns about installation and maintenance costs, as well as the perceived risk of rooftop water infiltration [54].

At the same time, the long-term economic benefits of green roofs are often underestimated. Green roofs can protect underlying roof layers from excessive thermal fluctuations, thereby extending the lifespan of waterproofing membranes from approximately 20 to 50 years and reducing maintenance requirements over time [55]. Nevertheless, the considerable structural load associated with intensive green roofs remains a major constraint for their implementation in existing buildings [56].

Economic analyses of green roofs and green walls are generally dominated by direct installation and maintenance costs, while intangible benefits, such as improvements in well-being and perceived environmental quality, are rarely included in return-on-investment assessments [57]. Nevertheless, studies do exist reporting that building-integrated vegetation technologies can positively affect property values [58]. For instance, Bianchini and Hewage reported that extensive and intensive green roofs can increase property values by approximately 2–5% and 5–8%, respectively [59]. Furthermore, green roof installation has been associated with increases of up to 16% in building rental prices [60], thereby representing a potential driver for the wider diffusion of building-integrated vegetation technologies.

Recent studies have extended this line of inquiry to assess the resilience of green façades under projected climate scenarios. For instance, Dehghan et al. (2025) analysed green walls in Turin under 2050 climate projections and found improvements in outdoor thermal comfort—with reductions in the universal thermal climate index by 0.55 °C—and a significant decrease in summer carbon emissions despite increased winter heating loads [61]. Similarly, Chew et al. (2023) identified climate-induced risks for green façades in tropical climates, including material degradation and reduced structural integrity due to increased temperature, rainfall, and wind stress [62]. In hot and dry climates such as Qatar, Andric et al. (2020) found that while green walls and roofs provided only modest energy savings (~3%), their broader benefits—including improved air quality and reduced UHI effects—justify their integration into climate adaptation strategies, especially when combined with insulation and efficient glazing [63]. In Egypt, Fahmy et al. (2017) applied a coupled outdoor–indoor simulation methodology to assess the performance of green façades and roofs under future climate scenarios. Their findings showed that while energy savings declined under more extreme future conditions, strategic placement of vegetation and increased green coverage still resulted in up to 21.3% energy cost savings and thermal comfort improvements in dense urban areas [64]. Further confirming these results, a study by Fahmy et al. (2020) demonstrated that urban canopy green coverage—particularly green façades—can lower indoor temperatures by up to 2.04 °C and reduce HVAC energy consumption by 6–7% in Egyptian suburban residential developments under future climate conditions (2020, 2050, and 2080) [65]. These findings emphasise the need for future-oriented façade design strategies that balance cooling efficiency with durability and resilience under intensified climatic stresses.

Despite increasing recognition of the role of nature-based strategies in climate adaptation, simulation-based studies quantifying the performance of green walls under future climate conditions remain relatively scarce. This study aims to address this gap by investigating the energy efficiency and climate resilience of green façades in the Italian residential building sector under future climate conditions, with a focus on the long-term trend dimension of climate resilience. Green façades—based on climbing plants supported by a vertical structure—were selected as the focus of this study because they are commonly used in retrofitting strategies due to their low maintenance and installation costs [66]. The analysis applies detailed mathematical modelling of the green façade within the Energy Plus simulation environment to assess a representative archetype of the Italian single-family houses built in the period 1946–1960. Two distinct climate zones in Italy—Rome and Turin—are considered across three time periods: the 2020s (2001−2020), 2050s (2041–2060), and 2090s (2081–2100).

Green façades are examined in various application scenarios, including different wall orientations, alongside a parametric evaluation of several building components under current energy efficiency regulations. Future typical meteorological years (TMYs) are used to reflect evolving climate conditions and to support a consistent long-term comparison of energy need and thermal comfort under climate change. They are suitable for this comparative purpose because they represent typical annual climate conditions. This focus does not undermine the relevance of extreme or semi-extreme weather events, which remain a complementary dimension of climate-resilience assessment. The performance is assessed through key performance indicators (KPIs), including weighted hours of exceedance beyond thermal comfort thresholds and annual thermal energy need for space heating and cooling. This integrated assessment provides a robust basis for

evaluating the potential of green façades to enhance long-term building performance and support climate resilience in urban environments.

2. Materials and methods

2.1. Green façade

Green walls are vegetative systems integrated into building envelopes that can provide multiple benefits, such as an increase in external wall thermal insulation, shading, evapotranspiration, and wind shielding (e.g., [67,68]). These mechanisms, in turn, influence both building energy consumption and urban microclimate [34].

Green walls are generally categorised into two main categories: green façades and living walls, each encompassing a range of configurations. Typically, green façades are characterised by a growing medium horizontally positioned and vegetation growing vertically adherent to the building envelope (direct green façade) or supported by structures, such as trellises, spaced away from the building walls (indirect green façade). Due to their simple structure, green façades can be easily installed on building exteriors.

By contrast, living walls feature an engineered substrate vertically positioned on building façades, either attached or detached from the building envelope [25]. Living walls are more complex than green façades, as they include an irrigation system and can be continuous or modular, depending on the type of support on which plants are grown [69].

Additionally, green façades are generally more cost-effective than living walls [70]. Direct greening systems typically range from 30 to 45 €/m^2 [71,72]. In a comprehensive review, Manso et al. [73] reported that the average construction cost of living walls is approximately 750 €/m^2. The same study estimated annual maintenance costs to average around 5.6 €/m^2/year for green façades and 19 €/m^2/year for living walls. However, green wall systems are influenced by several factors that can significantly affect both installation and maintenance costs, including water availability and the level of technological complexity adopted. Furthermore, ongoing advances in construction technologies may improve the overall cost-effectiveness of green wall solutions, as highlighted in recent studies [74]. Therefore, the widespread implementation of green façades in urban areas may require lower investments, making them a more feasible solution for potentially reducing UHI and building energy demands, depending on various factors.

Two primary mechanisms are critical when considering green facades:

1. Shading provided by vegetation can reduce solar radiation by approximately 70–95%.
2. Between 20 and 40% of the incoming solar radiation is used for evapotranspiration, which promotes air cooling [75].

Specifically, a study carried out by Bakhshoodeh et al. [76] focused on Perth, Australia, in a Mediterranean climate during hot weather conditions, showed that the mean contribution of evapotranspirative cooling to the overall cooling effect of the green façades was approximately 35% for deciduous plants and 25% for non-deciduous plants. These findings highlight the predominant role of shading in reducing façade surface temperatures.

2.2. Mathematical model and simulation framework of green façade (GF)

To evaluate the thermal effects of green façades on building envelopes, a Dynamic Heat Transfer (DHT) model was implemented, following the approach outlined by Zhang et al. [77]. The model integrates the Beer–Lambert law for shortwave radiation attenuation and the Penman–Monteith equation for estimating evapotranspiration, capturing both radiative and convective interactions between vegetation, wall surfaces, and the ambient environment.

The energy balance on the vegetated external wall surface accounts for four primary heat flux components: net solar radiation (q_{sw}), net longwave radiation (q_{lw}), convective heat flux (q_{conv}), and conductive heat flux (q_{cond}):

$$q_{sw} + q_{lw} + q_{conv} + q_{cond} = 0 \tag{1}$$

Shortwave radiation is affected by the vegetation transmittance (τ_v) and the wall absorptance (α_w), while the net longwave radiation accounts for emission and transmission through vegetation and interaction with the sky, ground, and air [77,78].

The vegetation energy balance includes net absorbed shortwave radiation ($q_{sw,v}$),net longwave radiation exchange ($q_{lw,v}$), convective heat exchange ($q_{conv,v}$), and latent heat flux from transpiration (q_{evap}):

$$q_{sw,v} + q_{lw,v} + q_{conv,v} + q_{evap} = 0 \tag{2}$$

Due to the nonlinear T^4 terms, the model is linearised during the simulation using a first-order expansion around the previous timestep to enable the solution of the equations.

To integrate this model with EnergyPlus, two Python Plugins were developed by authors to inject an additional heat source term:

$$q_{add} = (q_{sw} + q_{lw})_{GF} - (q_{sw} + q_{lw})_{bare} \tag{3}$$

The additional heat source (q_{add}) is computed at each simulation timestep and provided to EnergyPlus as a boundary condition on the external wall surface. The first term represents the net shortwave and longwave radiation fluxes acting on the wall in the presence of the green façade ($(q_{sw} + q_{lw})_{GF}$), while the second term represents the same fluxes on the uncovered bare wall ($(q_{sw} + q_{lw})_{bare}$). The difference between these two terms captures the net thermal effect of the vegetation layer on the external wall surface heat balance.

Fig. 1 shows the interaction between EnergyPlus and the Python Plugin Green Façade module.

The plugin was developed and described in detail in Nesci et al. [66], where the complete theoretical description of the mathematical model and its implementation are provided. The underlying mathematical model is based on the Dynamic Heat Transfer (DHT) model of Zhang et al. [77], where the model was experimentally validated against field measurements conducted on real green façades in Guangzhou, China, under hot-summer/warm-winter climate conditions. The validation compared simulated and measured values of solar and longwave radiation, vegetation temperature, and external wall surface temperatures. The maximum mean percentage error (MPE), mean bias error (MBE), and root mean square error (RMSE) were 1.61%, 0.45 °C, and 0.75 °C, respectively, demonstrating the high accuracy and low uncertainty of the model [77].

2.3. Key performance indicators

To assess the climate resilience of buildings under changing climatic conditions, four KPIs were selected, addressing both thermal comfort and energy performance. These indicators are drawn from the official KPI set adopted in IEA-EBC Annex 80 [79] and were chosen based on two main criteria: a) their capacity to capture thermal discomfort during free-floating conditions (i.e., in the absence of active space cooling or during power outages), and b) their effectiveness in evaluating the thermal performance of the building fabric under both cooling and heating operations. The definitions and assessment methods of all selected indicators are derived from the international technical standards.

The first KPI is the Hours of Exceedance (*HE*), which represents the number of hours during which the operative temperature in the zone exceeds the upper boundary of the acceptable indoor thermal comfort range. This indicator captures the frequency of thermal discomfort under free-floating conditions and is based on the adaptive comfort

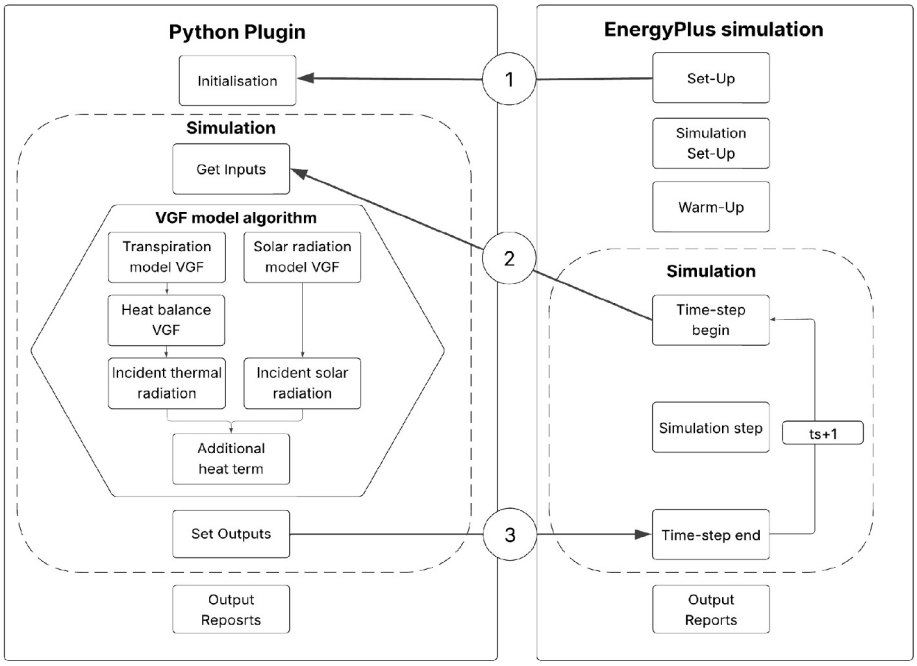

Fig. 1. Interaction between the EnergyPlus and Python green façade module. (For interpretation of the references to colour in this figure legend, the reader is referred to the web version of this article.)

model defined in Annex H.2 of ISO 17772-1 [80]. The second KPI is the Weighted Hours of Exceedance (*WHE*), an extension of *HE* that incorporates the severity of each exceedance. Each hour is weighted according to the magnitude of deviation from the comfort threshold, following EN ISO 7730 (Method B) [81]. This provides a more detailed representation of warm discomfort by integrating both intensity and duration.

The third and fourth KPIs are the thermal energy needs for space cooling and heating per unit conditioned floor area ($EP_{C,nd}$ and $EP_{H,nd}$ (kWh·m^{-2})). The terminology "need" is adopted following ISO 52000-1:2017 [82]. These indicators reflect the building's basic energy need under ideal thermal conditions—namely, a uniform and optimally controlled indoor temperature, without the influence of specific technical building systems. The energy needs are calculated under simplified conditions, assuming purely convective heat emission and continuous system operation without power [83].

Including space heating energy need among the selected KPIs allows for a balanced evaluation of the building's thermal performance across all seasons. Green façades can influence winter conditions depending on their design (e.g., deciduous vs. evergreen vegetation), orientation, and climatic context—either by providing additional insulation or by reducing beneficial solar gains. Therefore, accounting for heating need supports the identification of seasonal trade-offs and contributes to a more comprehensive assessment of the building's year-round thermal resilience.

The specific vegetation parameters adopted for the green façade model (e.g., leaf area index, leaf transmittance) were selected to represent practical and well-established deciduous climbing systems suitable for the Italian context; a detailed justification of these assumptions is provided in Section 3.3.

3. Case study

3.1. Building description

The methodology was applied to a representative Italian single-family house constructed between 1946 and 1960. This case study was selected from a set of archetypes developed under the CIP-IEE-2008 -TABULA research project [84]. This typology-based approach supports the development of bottom-up energy models, enabling results to be scaled from a representative archetype to the broader building stock [85,86]. Buildings from this construction period offer substantial energy-saving potential compared to other periods [86,87], making this archetype particularly relevant for investigating climate resilience and energy efficiency improvements. Moreover, the single-family house presents a high sensitivity to climate change due to its high shape factor ($A_{env}/V_g = 0.73$ m^{-1}) [88]. The building model was assessed in two distinct climatic zones, represented respectively by Rome and Turin. The selected archetype and climatic contexts concern a substantial and relevant part of the national stock. According to the last available census data [89], approximately 51% of the total Italian residential buildings contain only one dwelling and can therefore be regarded as single-family residential buildings. The selected locations also represent two of the most widespread Italian climatic conditions. Rome belongs to climatic zone D, whereas Turin belongs to climatic zone E. National building-stock analyses indicate that zones D and E together contain approximately three quarters of Italian residential buildings, covering overall 73% of the Italian municipalities and 71% of the Italian population. The case study was assessed under three climatic scenarios, as detailed in Section 3.3.

The case study was modelled considering two configurations: a pre-retrofit variant, representing the building in its original state, and a post-retrofit variant reflecting a refurbished version. In the pre-retrofit variant, the case study presents envelope technologies that are typical of its construction period, i.e., solid brick masonry walls and single-glazed windows, in accordance with TABULA.

3.2. Retrofit measures

In the post-retrofit variant, the building envelope is refurbished to comply with the minimum energy performance requirements set by the Italian national regulations for the reference building in different climatic zones [90]. The thermal transmittance and areal heat capacity values of the envelope components for both pre- and post-retrofit variants are reported in Table 1 for each site. The areal heat capacity values show that the addition of the insulation layer during retrofit contributes

Table 1
Thermal transmittance and areal heat capacity values of the building envelope components of the case study.

Building components	Pre-retrofit building variant		Post-retrofit building variant			
	Turin and Rome		Turin		Rome	
	U-value [W·m^{-2} K^{-1}]	*K*-value [KJ·m^{-2} K^{-1}]	*U*-value [W·m^{-2} K^{-1}]	*K*-value [KJ·m^{-2} K^{-1}]	*U*-value [W·m^{-2} K^{-1}]	*K*-value [KJ·m^{-2} K^{-1}]
Opaque walls	1.48	559	0.26	564	0.29	562
Roof	2.20	452	0.22	457	0.26	455
Bottom floor	2.00	489	0.26	494	0.29	492
Windows	4.90	–	1.40	–	1.80	–

negligible thermal mass, leaving the thermal inertia of the building envelope virtually unchanged between pre- and post-retrofit conditions.

Additionally, for the post-retrofit variant, the building was equipped with movable solar shading devices, consisting of external wooden Venetian blinds; under this configuration, the value of the total solar energy transmittance of the system glazing *plus* shading, g_{gl+sh}, is equal to 0.15. In the model, the blinds are activated when the beam plus diffuse solar irradiance incident on the window exceeds 300 W·m^{-2} [91].

To better assess the specific effect of the green façade, a ventilative cooling system was integrated in the post-retrofit variant to further mitigate the risk of summer overheating due to insulation, which amplifies indoor cooling loads. The system was implemented through EnergyPlus's Energy Management System (EMS) by dynamically adjusting the air change rates (ACH), based on thermal conditions, to maximize the benefits of nighttime cooling and support comfort during transitional seasons. In free-floating mode, ventilative cooling was activated when the indoor operative temperature exceeded the upper adaptive comfort limit, and the indoor air temperature was at least 2 °C higher than the outdoor temperature. The system was deactivated when the operative temperature fell below the lower adaptive limit or when the indoor temperature dropped below the outdoor temperature. Under ideal load conditions, activation occurred whenever a cooling load was detected, and the indoor air temperature exceeded the outdoor air temperature by at least 2 °C. Deactivation was triggered when no cooling load was present or when the indoor temperature was lower than the outdoor temperature. In both cases, the ACH was set to 3 h^{-1} during activation and reduced to 0.2 h^{-1} when deactivated.

The chosen air exchange rate during the activation of ventilative cooling was determined using the Ventilative Cooling Potential Tool (VC Tool), developed within the IEA-EBC Annex 62 project [92]. To assess the extent to which ventilative cooling can offset cooling loads, the VC Tool estimates the energy contribution of ventilative cooling by analyzing a single-zone energy balance, assuming a well-mixed indoor air volume, and accounting for building envelope thermal properties, internal heat gains, ventilation requirements, and occupancy patterns. In this study, direct cooling through increased airflow was considered when the outdoor air temperature was at least 2 °C lower than the indoor air temperature. This threshold follows the recommendations of the Ventilative Cooling Design Guide [93] developed under Annex 62. Additionally, the thermal effect of fan energy consumption was accounted for by increasing the inlet air temperature by an average of 0.4 °C. The Specific Fan Power (SFP) was set at 1.08 kW·m^{-3}s, under the Italian reference building regulations [90]. When the conditions for ventilative cooling were not met—as well as in all pre-retrofit cases—the ACH was set equal to the minimum value required for indoor air quality as specified in the draft Italian National Annex of EN 16798–1 [94].

3.3. Modelling configurations and assumptions

The green facade scenarios were applied to both pre- and post-retrofit building variants. The analysis explores different green façade orientations, beginning with greenery coverage limited to the South-facing façade, and then expanding to a multi-orientation configuration, encompassing the South, East, and West façades. The different simulation configurations are summarised in Fig. 2, which presents the cases analysed in this study.

The green façade was modelled assuming deciduous climbing vegetation with 100% façade coverage. The adopted configuration is representative of indirect green façade systems based on climbing vegetation supported by cables or trellis structures, consistently with the typology described in Section 2.1 [95]. The assumed vegetation type is representative of common deciduous climbing species widely used in green façade applications in Italian and Mediterranean contexts, such as *Parthenocissus tricuspidata* and *Wisteria sinensis* [95–97]. A monthly variable LAI between 1 and 5 was used to reproduce the seasonal growth cycle of the vegetation with lower values in winter and maximum foliage development in summer. The chosen LAI range is within the recommended range for deciduous climbing plants (1.0–6.0) and consistent with previous studies on green façades in Mediterranean and temperate climates [77] where LAI was found to be one of the main parameters controlling shading and evapotranspirative cooling performance. A leaf transmittance value of 0.23 was assumed, obtained through spectral integration of leaf optical data based on the ISO 9050:2003 [98] to the implementation framework proposed by Zhang et al. [77] and adapted in Nesci et al. [66]. The dimension of the leaf was fixed at 0.10 m × 0.05 m. The minimum stomatal resistance was fixed at 100 s·m^{-1}, within the range of 50–300 s·m^{-1} consistent with literature values for the plant species considered [77]. Soil moisture was represented by a fixed average value, unchanged across time steps and climate scenarios. The model does not simulate a dynamic soil-water balance, VPD-induced stomatal closure, irrigation demand, plant mortality, or stress-related changes in LAI and vegetation coverage. The results therefore represent potential performance under maintained vegetation conditions.

Dynamic simulations were performed using EnergyPlus (version 23.2), integrated with a custom Python plugin designed to implement the mathematical model of the green façade. Standard user behavior was assumed across all simulations, with internal heat gains and occupancy profiles also defined according to the same reference. To assess the thermal energy needs for space cooling and space heating, an ideal load system was assumed under EN ISO 52016-1 [83], with infinite power and purely convective thermal load.

The analyses focused on two Italian cities: Rome and Turin, belonging, respectively, to ASHRAE climate zones 3 A (Warm Humid) and 4 A (Mixed Humid) [99], and to Köppen–Geiger classification Csa (Hot-summer Mediterranean) and Cfa (Humid subtropical) [100].

To evaluate climate resilience, simulations were conducted using the Typical Meteorological Years (TMYs) for three timeframes: 2020s (2001–2020), 2050s (2041–2060), and 2090s (2081–2100). The weather files were generated following the approach developed by the IEA-EBC Annex 80 Weather Data Task Group [101]. For Rome, the TMYs were taken directly from the existing Annex 80 dataset. For Turin, the TMYs were generated specifically for this study, following the same Annex 80 methodology. This ensured consistency between the two cities in terms of time horizons, weather-file format and climate-data processing.

The weather files were based on Euro-CORDEX climate projections from the CMIP5 generation of climate models. Future climate conditions were represented under the Representative Concentration Pathway 8.5 (RCP 8.5), a high-emission scenario commonly used for conservative

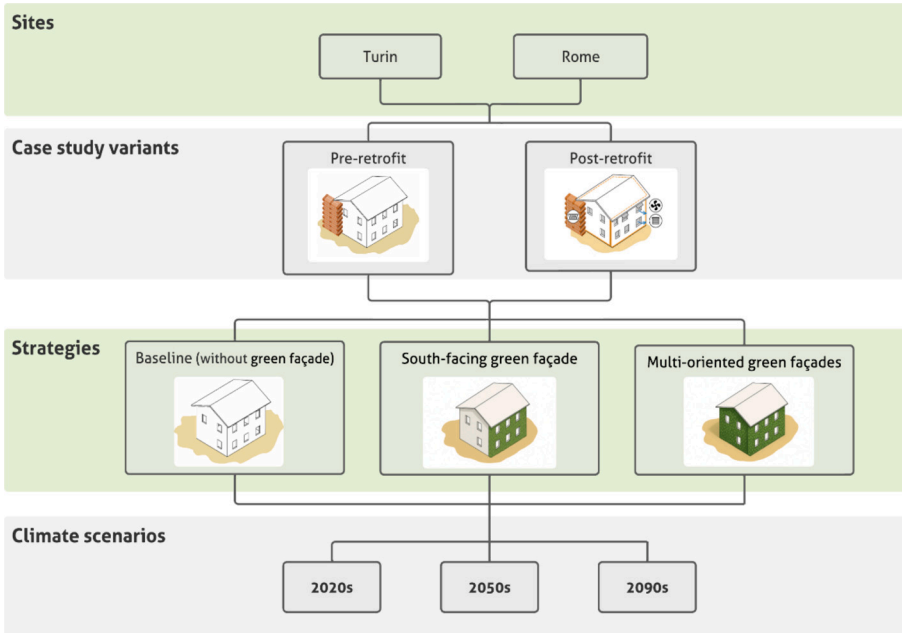

Fig. 2. Overview of the analysed configurations.

climate-resilience assessments. For the European cities, the dataset used MPI-ESM-LR as the driving global climate model and REMO as the regional climate model, with a spatial resolution of 0.11° (approximately 12.5 km). The projections were dynamically downscaled and then bias-corrected using Quantile Delta Mapping and Multivariate Bias Correction with N-dimensional Probability Density Function Transform. The bias correction was performed month by month using the available observational data for calibration, to preserve monthly variability and reduce systematic deviations between raw model outputs and local observations. The final files were prepared in EnergyPlus Weather File (EPW) format for dynamic building simulation.

Table 2 summarises the average values of air temperature, specific humidity, and global horizontal solar irradiance in June, July, and August for both sites, highlighting the changing trends over time. While air temperature and specific humidity show increasing trends for both cities across all future scenarios, the global horizontal solar irradiance follows opposite trends in the two cities, increasing in Rome and decreasing in Turin. This divergence is physically consistent with Euro-CORDEX projections for northern Italy, where increased atmospheric moisture and cloud cover associated with future warming are projected to reduce surface solar radiation [102,103], in contrast to central and southern Italy where solar radiation is projected to increase.

4. Results

The effect of green façade deployment on indoor thermal comfort performance is evaluated using Hours of Exceedance (*HE*) and Weighted Hours of Exceedance (*WHE*), which account for both the frequency and severity of thermal discomfort. In addition, energy performance implications were evaluated by analyzing the building's cooling and heating needs. Results are provided for both "pre-retrofit" and "post-retrofit + ventilative cooling" configurations, across Rome and Turin, under three climatic scenarios—2020s, 2050s, and 2090s—and for three façade typologies: baseline (i.e., bare façade), South-facing green façade, and multi-oriented green façades. The complete set of results for all configurations is provided in the tables in Appendix A.

4.1. Thermal comfort performance

In Rome, under the 2020s climatic scenario, and in pre-retrofit condition, the baseline case shows 1877 *HE* and 3475 *WHE*, as displayed in Fig. 3(a) and Table A.1. Implementing a South-facing green façade leads to 1760 *HE* and 2989 *WHE*, equal to a reduction of 6.2% and 14.0%, respectively. The impact is much greater with the multi-oriented green façades configuration, which limits discomfort to 834 *HE* (−55.6%) and 1094 *WHE* (−68.5%), thereby demonstrating the superior mitigation potential of full façade coverage. This trend persists under future climate scenarios. For instance, in the 2050s, the South-facing green façade configuration reduces *HE* by 8.1% and *WHE* by 13.2%, while in the 2090s, the reductions, compared to the baseline case, are 3.8% for *HE* and 8.9% for *WHE*. In contrast, the multi-oriented green façades configuration achieves a 32.8% reduction in *HE* and 51.6% in *WHE* in the 2050s and maintains notable performance in the 2090s with reductions of 27.1% and 39.6%, respectively.

In Turin, pre-retrofit results show similar benefits (Fig. 4(a) and Table A.2). Under the 2020s climate scenario, the baseline case yields 747 *HE* and 1103 *WHE*. The application of a South-facing green façade reduces *HE* to 552 (−26.1%) and *WHE* to 769 (−30.3%), while multi-oriented green façades lower the *HE* to 135 (−81.9%) and *WHE* to 170 (−84.6%). These improvements persist in projected climates, confirming the long-term comfort benefits of façade greening, especially under future warming scenarios. The South-facing façade provides a

Table 2
Average climate variables for Rome and Turin during June, July, and August across the three climate scenarios (2020s, 2050s, 2090s).

Climate variable	Air temperature [°C]			Specific humidity [$g_v \cdot kg_a^{-1}$]			Global horizontal solar irradiance [$W \cdot m^{-2}$]		
Climate scenarios	2020s	2050s	2090s	2020s	2050s	2090s	2020s	2050s	2090s
Rome	24.4	26.3	28.9	13	13.7	15.9	309.4	309.5	310.6
Turin	23.1	24.2	27.1	8.1	11.9	12.7	253.6	251.4	248.2

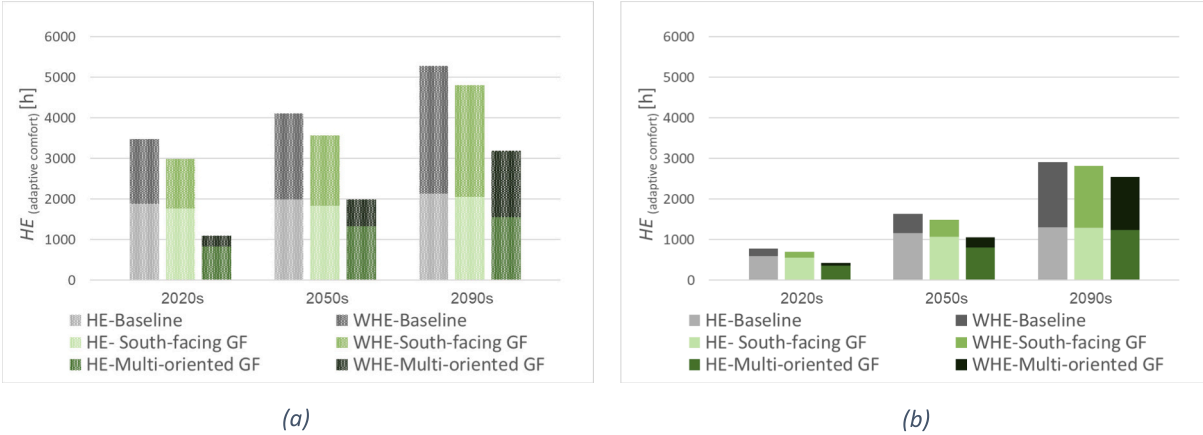

Fig. 3. Thermal comfort indicators in Rome for pre-retrofit (a) and post-retrofit (b) in the 2020s, 2050s, and 2090s.

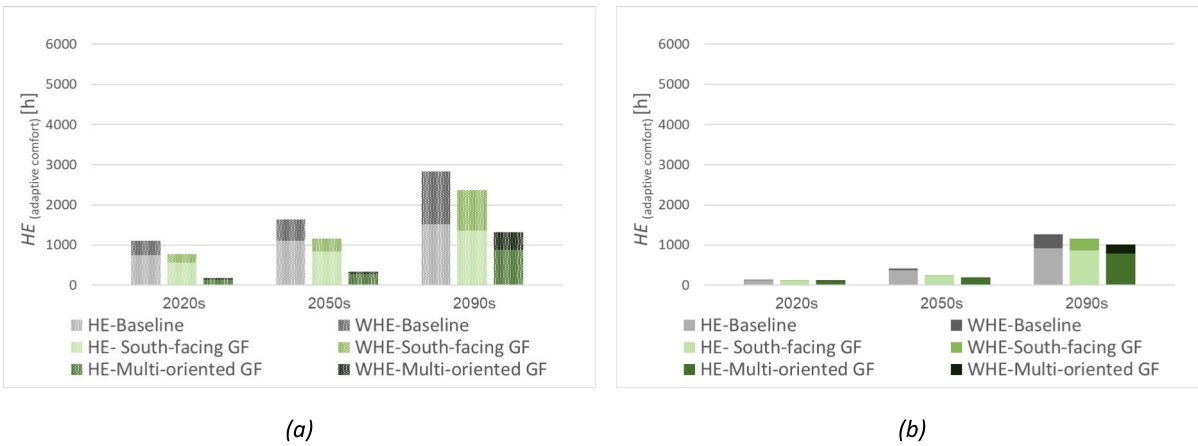

Fig. 4. Thermal comfort indicators in Turin for pre-retrofit (a) and post-retrofit (b) in the 2020s, 2050s, and 2090s.

reduction of *HE* by 24.3% and 10.5%, and of *WHE* by 29.5% and 16.5%, for the 2050s and 2090s, respectively. As in Rome, results indicate that in Turin, the more the climatic scenarios are projected into the future, with an increase in the discomfort hours of the baseline case, the smaller, though still relevant, is the effectiveness of adopting green facades.

In post-retrofit conditions, Rome's baseline (i.e., 2020s) *HE* drops from 1877 (pre-retrofit) to 592 (post-retrofit) (−68.5%), due to envelope retrofit and ventilative cooling (Fig. 3(b) and Table A.3). The South-facing green façade further reduces *HE* to 551 (−6.9%) and *WHE* to 701 (−9.4%), while multi-oriented green façades achieve more substantial reductions compared to the post-retrofit baseline case: 359 *HE* (−39.4%) and 416 *WHE* (−46.3%). The relative contribution of green façades to comfort improvement becomes more pronounced in post-retrofit conditions due to the lower absolute baseline. This pattern is consistent across future climate scenarios. Under the 2050s scenario, the South-facing GF provides relative performance quite like that of the 2020s, with the percentage reduction in *WHE* unchanged. In comparison, the multi-oriented GFs deliver for both *HE* and *WHE* approximately 10% lower reductions than those observed in the 2020s. In the 2090s, the baseline in Rome shows *HE* rising to 2139 (pre-retrofit) and 1310 (post-retrofit). In the post-retrofit condition, the South-facing GF leads to a slight improvement (1288 *HE*, −1.7%, and 2818 *WHE*, −3.0%), suggesting limited effectiveness as climatic extremes intensify. The multi-oriented GFs still perform notably better, reducing *HE* to 1232 (−6.0%) and *WHE* to 2539 (−12.6%), with a percentage reduction performance significantly lower than for the 2020s or 2050s, but still offering meaningful gains, i.e., an absolute reduction of 367 weighted discomfort hours.

In 2020s in Turin, retrofit improvements reduce *HE* from 747 to 125. As shown in Fig. 4(b) and Table A.4, the addition of a South-facing GF further improves performance, lowering *HE* to 102 (−18.4%) and *WHE* to 109 (−19.3%), while the multi-oriented GFs configuration provides a slightly greater reduction, with *HE* decreasing to 101 (−19.2%) and *WHE* to 107 (−20.7%). These reductions, while numerically small, still contribute to occupant comfort. Under the 2050s climate scenario, discomfort increases considerably, with the baseline case's *HE* rising to 366 and *WHE* to 416. The South-oriented GF reduces *HE to* 221 (−39.6%) and *WHE* to 240 (−42.3%), while the multi-oriented GFs result in 175 *HE* (−52.2%) and 188 *WHE* (−54.8%). By the 2090s, the baseline case reaches discomfort levels of 912 *HE* and 1256 *WHE*. The South-facing GF configuration achieves reductions to 858 *HE* (−5.9%) and 1161 *WHE* (−7.6%), indicating only modest gains under more intense climatic stress. However, multi-oriented GFs still maintain a valuable contribution, lowering *HE* to 781 (−14.4%) and *WHE* to 1009 (−19.7%); although the relative improvement is smaller than in the 2050s scenario, the absolute reduction in discomfort hours remains important for thermal resilience.

4.2. Energy performance

In the pre-retrofit condition for Rome, under the 2020s climate scenario, the baseline cooling need is 32.1 kWh·m^{-2} and heating need is 57.0 kWh·m^{-2}, as shown in Fig. 5(a) and in Table A.5. The South-facing green façade configuration decreases the cooling need to 27.2 kWh·m^{-2}, corresponding to a 15.3% reduction. However, heating need rises to

Fig. 5. Thermal energy needs for space heating and cooling in Rome for pre-retrofit (a) and post-retrofit (b) in the 2020s, 2050s, and 2090s.

64.5 kWh·m^{-2}, marking a 13.2% increase. This is expected, as vegetation on the South façade reduces wintertime solar gains. The multi-oriented green façades achieve an even more pronounced reduction in cooling need, lowering it to 15.7 kWh·m^{-2}, equal to a decrease of 51.1% compared to the baseline case. Conversely, this configuration increases heating need up to 74.3 kWh·m^{-2} (+30.4%). In the 2050s climate scenario, the baseline cooling need rises significantly to 42.8 kWh·m^{-2} as climate change intensifies summer temperatures. The South-facing GF configuration reduces this to 36.7 kWh·m^{-2} (−14.3%), while multi-oriented GFs bring it down to 22.8 kWh·m^{-2} (−46.7%). However, both configurations are associated with an increase in heating energy need: from 35.2 kWh·m^{-2} in the baseline case to 41.2 kWh·m^{-2} (+17.0%) for the South-facing GF and to 48.3 kWh·m^{-2} (+37.2%) for the multi-oriented configuration. Despite this increase, the net energy balance remains favourable, as the reduction in cooling need outweighs the rise in heating need. By the 2090s, the baseline cooling need reaches its maximum value of 65.0 kWh·m^{-2}, reflecting the impact of extreme warming. The South-facing GF reduces this to 57.8 kWh·m^{-2} (−11.1%), while multi-oriented GFs provide the most considerable savings at 40.7 kWh·m^{-2} (−37.4%). Meanwhile, heating need drops to 14.9 kWh·m^{-2} in the baseline case, increasing to 19.0 kWh·m^{-2} (+27.5%) with south-facing coverage and to 23.6 kWh·m^{-2} (+58.4%) with multi-oriented greening. These results highlight a shift in energy needs, with cooling need becoming dominant as winter heating becomes less relevant.

In Turin, the pre-retrofit baseline case under the 2020s climate scenario shows a cooling need of 13.5 kWh·m^{-2}, with heating of 112.6 kWh·m^{-2}, shown in Fig. 6(a) and in Table A.6. The South-facing GF reduces cooling to 10.4 kWh·m^{-2} (−23.0%) while increasing heating to 121.3 kWh·m^{-2} (+7.7%). The multi-oriented GFs perform even better in terms of cooling, reducing the need to just 5.5 kWh·m^{-2} (−59.3%), but this comes with a significant heating penalty, raising the need to 128.5 kWh·m^{-2} (+14.2%). This trade-off underscores the importance of context-specific façade strategies, particularly in climates with substantial winter heating needs.

In the 2050s, cooling need increases to 18.8 kWh·m^{-2}. Green façades continue to mitigate this rise: the South-facing GF reduces it to 15.2 kWh·m^{-2} (−19.1%), and the multi-oriented GFs configuration further cuts it to 9.3 kWh·m^{-2} (−50.5%). Heating need increases from 100.0 kWh·m^{-2} (baseline) to 108.1 kWh·m^{-2} (+8.1%) with South-facing GF and 114.9 kWh·m^{-2} (+14.9%) with multi-oriented GFs. In the 2090s climate scenario, the baseline cooling need rises to 36.1 kWh·m^{-2}. The South-facing green façade brings this down to 30.3 kWh·m^{-2} (−16.0%),

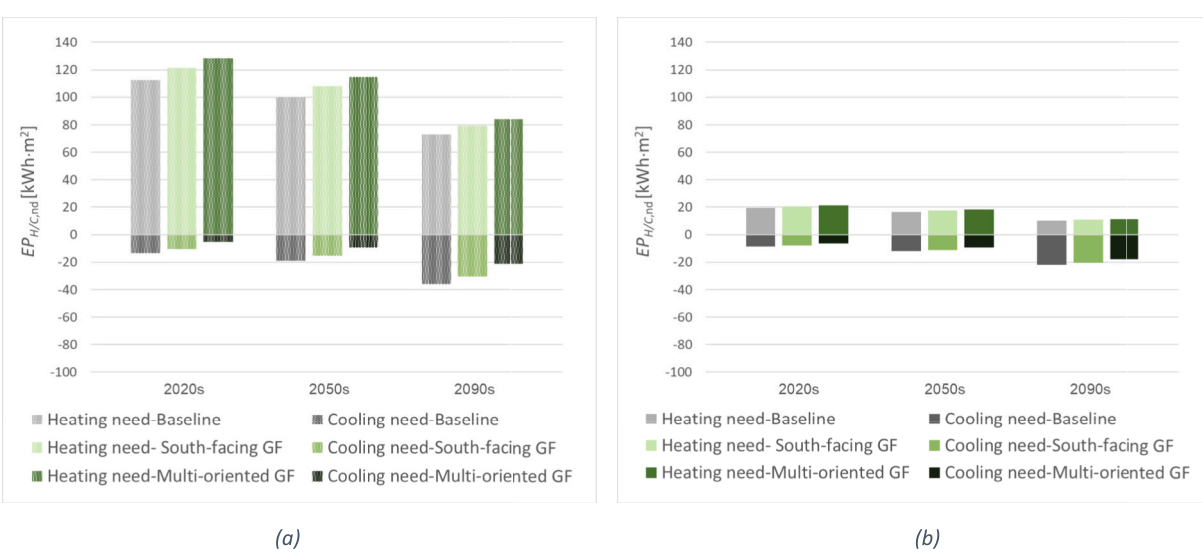

Fig. 6. Thermal energy needs for space heating and cooling in Turin for pre-retrofit (a) and post-retrofit (b) in the 2020s, 2050s, and 2090s.

while multi-oriented GFs reduce it to 21.1 kWh·m^{-2} (−41.5%). Meanwhile, heating need drops due to milder winters, and the increase due to greenery is consistently smaller than in previous climate scenarios: from 72.8 kWh·m^{-2} in the baseline case to 79.3 kWh·m^{-2} (+8.9%) with South-facing greening, and 83.9 kWh·m^{-2} (+15.1%) with multi-oriented coverage. Although the heating penalty persists, its absolute magnitude diminishes, while cooling savings grow more substantial over time.

In the post-retrofit condition for Rome, for the 2020s, the baseline cooling need drops from 32.1 to 19.0 kWh·m^{-2} due to the retrofit, shown in Fig. 5(b) and in Table A.7. The addition of a South-facing GF further reduces this to 17.9 kWh·m^{-2} (−5.8%), while the multi-oriented configuration lowers it to 14.7 kWh·m^{-2} (−22.6%). On the other side, heating need, already reduced from 57.0 to 8.1 kWh·m^{-2}, increases to 9.1 kWh·m^{-2} (+12.3%) with South-facing greening and to 10.5 kWh·m^{-2} (+29.6%) with full façade coverage. In the 2050s, the post-retrofit baseline cooling need reaches 26.0 kWh·m^{-2}, the South-facing GF cuts this to 24.6 kWh·m^{-2} (−5.4%), and the multi-oriented scenario to 20.5 kWh·m^{-2} (−21.2%). Heating need remains small, increasing from 2.4 to 2.9 (+20.8%) and 3.6 kWh·m^{-2} (+50%) respectively. Despite these relative increases, the absolute values remain low, and the net annual energy impact favors façade greening.

In the 2090s, Rome's baseline cooling need increases sharply to 37.5 kWh·m^{-2} due to climate warming. The South-facing green façade provides limited relief (−4.3%), lowering the need to 35.9 kWh·m^{-2}, whereas multi-oriented GFs reduce it to 31.3 kWh·m^{-2} (−16.5%). The heating need is negligible, remaining near zero in all scenarios.

In the post-retrofit condition for Turin, in the 2020s, the baseline cooling need falls from pre-retrofit's 13.5 kWh·m^{-2} to 8.5 kWh·m^{-2}, as shown in Fig. 6(b) and in Table A.8. A South-facing green façade reduces this to 7.8 kWh·m^{-2} (−8.2%), while multi-oriented façades lower it further to 6.4 kWh·m^{-2} (−24.7%). The heating need, reduced from 112.6 to 19.5 kWh·m^{-2} by the retrofit strategies, increases slightly to 20.4 kWh·m^{-2} (+4.6%) and 21.2 kWh·m^{-2} (+8.7%), under the two green facade configurations respectively. Anyhow, this increase remains lower than the cooling gains achieved. In the 2050s, with warmer summers and milder winters, cooling needs reach 12.0 kWh·m^{-2} in the baseline scenario. South-facing GFs reduce this to 11.1 kWh·m^{-2} (−7.5%) and multi-oriented GFs to 9.4 kWh·m^{-2} (−21.7%). Heating grows slightly from 16.4 kWh·m^{-2} to 17.5 kWh·m^{-2} (+6.7%) and 18.2 kWh·m^{-2} (+11.0%), respectively, with the heating penalty increasingly offset by the summer savings. In the 2090s, the baseline case cooling need peaks at 21.8 kWh·m^{-2}. The South-facing green façade cuts this to 20.4 kWh·m^{-2} (−6.4%), while the multi-oriented option brings it down to 18.0 kWh·m^{-2} (−17.4%). Heating need grows modestly from 10.1 kWh·m^{-2} to 10.9 kWh·m^{-2} (+7.9%) and 11.4 kWh·m^{-2} (+12.9%), respectively. While the heating penalty persists, the absolute benefit in cooling performance continues to outweigh it, especially in the long-term climate scenarios.

To clarify the attribution of effects in the post-retrofit scenarios, the refurbished configuration without green façade is treated as the post-retrofit baseline. Table 3 summarises the additional marginal contribution of green façades beyond the retrofit package, which includes envelope insulation, solar shading and ventilative cooling.

Table 3
Summary of the additional marginal contribution of green façades in the post-retrofit scenarios, calculated with respect to the post-retrofit baseline without green façade.

City	Climate Scenarios	Strategies	*WHE* variation (−)	*EPC,nd variation* (−)	$EP_{H,nd}$ variation (−)
Rome	2020s	South-facing GF	−9.4%	−5.8%	12.3%
		Multi-oriented GF	−46.3%	−22.6%	29.6%
	2050s	South-facing GF	−9.4%	−5.4%	20.8%
		Multi-oriented GF	−35.8%	−21.2%	50.0%
	2090s	South-facing GF	−3.0%	−4.3%	0.0%
		Multi-oriented GF	−12.6%	−16.5%	0.0%
Turin	2020s	South-facing GF	−19.3%	−8.2%	4.6%
		Multi-oriented GF	−20.7%	−24.7%	8.7%
	2050s	South-facing GF	−42.3%	−7.5%	6.7%
		Multi-oriented GF	−54.8%	−21.7%	11.0%
	2090s	South-facing GF	−7.6%	−6.4%	7.9%
		Multi-oriented GF	−19.7%	−17.4%	12.9%

5. Discussion

The results presented in this study highlight the potential of green façades to enhance the climate-change resilience of residential buildings in the analysed Italian building stock segment. However, the effectiveness in improving thermal comfort and reducing cooling energy needs under current and future climate scenarios varies significantly depending on the climatic zone, building retrofit conditions, green façade orientation, and reference time horizon. This overall pattern is consistent with the literature: vertical greenery consistently improves summer comfort, with performance governed by multiple factors—most notably climate and façade exposure (orientation) [31,32,34,67].

Findings show that green façades reduce thermal discomfort, particularly when applied to multiple orientations. This highlights the benefits of covering multiple façades to reduce thermal stress, especially in pre-retrofit buildings with low envelope performance, where multi-oriented green façades reduce *WHE* by 68.5% in Rome and 84.6% in Turin under the 2020s climate scenario, and still achieve reductions of 39.6% and 53.2%, respectively, by the 2090s. The *WHE* reductions are compatible with reported 0.5–2.0 °C indoor temperature attenuation and fewer overheating hours for vertical greenery systems when adequate coverage is provided [30,67,69]. In addition, the observed advantage of multi-orientation over a single south-facing façade reflects that treating several orientations spreads shading and evapotranspiration across the day, thereby reducing peak solar heat gains [31,32,63].

In the post-retrofit condition, the integration of energy efficiency measures, including ventilative cooling, already leads to a substantial reduction in discomfort hours compared to the baseline, providing a strong baseline for further optimisation through green façades. In this context, green façades can still contribute meaningfully to further improvements. This reduction, for both types of green façade application, reaches its peak in the 2020s for Rome (up to 46.3%) and in the 2050s for Turin (up to 54.8%), with the application of multi-oriented green façades consistently outperforming South-facing green façades. These results further support the view that summer benefits persist even after retrofit actions, in agreement with experimental and numerical evidence on insulated façades [31,67]. Although the relative improvement diminishes under more extreme future scenarios like the 2090s, with reductions dropping from 46.3% in the 2020s to 12.6% in the 2090s in Rome and from 54.8% in the 2050s to 19.7% in the 2090s in Turin, the absolute reduction in discomfort hours avoided remains considerable, continuing to support the objective of long-term thermal resilience. This pattern aligns with climate-scenario analyses of overheating mitigation in the literature, which report significant absolute reductions in discomfort hours, even as the relative effectiveness declines under projected warming scenarios [2,4].

The decline in percentage effectiveness under future climates should not be attributed to VPD-induced stomatal closure, since this

physiological response is not represented in the model. Rather, it mainly reflects the increasing cooling and overheating baseline: green façades provide relevant—and in some cases increasing—absolute savings, although these correspond to smaller percentage reductions as the baseline load grows. In practice, maintaining the assumed performance may require drought-tolerant species, adequate irrigation and regular maintenance, particularly under the 2090s climate. [30,69]

From an energy performance perspective, the results confirm the substantial cooling energy savings achievable through the application of green façades in pre-retrofit buildings. In the 2020s, the cooling energy need in Rome decreases by 51.1%, and up to 59.3% in Turin, when multi-oriented green façades are implemented. These values lie at the upper end of the ranges (26–60% reductions in cooling energy for multiple-façade applications) reported for vertical greenery analyses in Mediterranean/warm-temperate contexts [31,34,69,75].

However, these cooling benefits are accompanied by increased heating needs, since the green façade also reduces useful solar gains in winter. To make this seasonal trade-off explicit, Tables A.5 to A.8 report, alongside the cooling and heating needs, the total annual thermal energy need of each configuration and its change with respect to the corresponding bare-wall baseline. This aggregate is computed at the building-demand level and does not account for the different energy carriers and system efficiencies of heating and cooling; it is therefore used here to compare the seasonal balance of the configurations, not as a primary-energy or cost indicator, which would require the techno-economic assessment identified as future work. The net annual balance depends strongly on climate and building state. In Rome pre-retrofit, the winter penalty nearly cancels the summer benefit under the current climate, where the multi-oriented configuration leaves the total annual thermal need almost unchanged (+1.0% in the 2020s), but the balance turns increasingly favourable as summers warm, reaching a 19.5% reduction by the 2090s. In Turin pre-retrofit, the higher baseline heating need dominates: the absolute winter penalty of the multi-oriented configuration outweighs the cooling saving under the current and mid-century climates, so the total annual thermal need increases (+6.3% in the 2020s and + 4.5% in the 2050s), and the balance becomes favourable only under the 2090s scenario (−3.6%). This confirms that, in colder climates with high heating demand, the annual benefit of green façades cannot be inferred from cooling savings alone. The picture is more favourable in the post-retrofit buildings, where insulation and solar control strongly reduce the heating need and therefore the absolute winter penalty: here the multi-oriented configuration lowers the total annual thermal need in almost all cases, by up to 16.3% in Rome and 7.8% in Turin. These results are consistent with reports that winter penalties concentrate on south-facing greening in colder climates when solar gains are reduced, while the net annual balance tends to remain favourable in warmer climates and in well-insulated buildings [63].

In Rome's post-retrofit scenarios, energy efficiency measures combined with ventilative cooling lead to significant reductions in both heating and cooling energy needs. Yet, green façades still offer additional energy benefits, especially in mitigating rising cooling needs projected in future climate scenarios. Accordingly, the post-retrofit reductions attributed to green façades should be interpreted as additional marginal benefits beyond envelope insulation, solar shading and ventilative cooling, rather than as the combined effect of the full retrofit package. For example, in the 2050s, multi-oriented green façades achieve a further 21.2% reduction in cooling needs, despite the already optimized baseline. These trends suggest that, under future climates, green façades remain a potentially effective solution for achieving a considerable relative reduction in annual cooling loads—especially in cities like Rome, where summer energy need is expected to rise sharply—despite the relatively smaller absolute energy savings in post-retrofit buildings. Comparable future-scenario studies likewise report persistent energy and comfort benefits (even as they decline towards the end of the century), corroborating the long-term value of façade greening when summer loads escalate [64,65].

Lastly, Turin's post-retrofit cooling energy results present a more balanced profile as green façades continue to support the reduction of cooling need by up to 24.7% in the 2020s, while introducing manageable heating penalties, especially as winters become milder in the future. This reinforces the value of green façades as a climate-adaptive retrofit solution, capable of supporting both energy savings and thermal comfort goals in future residential building design.

Furthermore, the results obtained for green façade applications should be interpreted with reference to the specific building archetype adopted in the simulations, which does not include balconies. Different, and potentially less favourable, outcomes may be obtained for buildings with different geometries or façade configurations, such as those incorporating balconies. A key aspect affecting the long-term performance of green façades is maintenance. The simulations assumed full vegetation coverage of all available façade surfaces (excluding openings), corresponding to plants in good health and supported by adequate irrigation. Consequently, maintenance requirements, irrigation needs, and the costs associated with plant replacement represent critical factors influencing the effectiveness of the system [104]. Fire safety is also closely linked to maintenance: recent studies have shown that healthy and well-maintained vegetation can exhibit self-extinguishing behavior, whereas dry or poorly maintained plants may increase fire risk [105,106]. Therefore, fire safety considerations should be addressed within the broader framework of vegetation management and maintenance practices. Although green façades entail installation and maintenance costs throughout their service life, these costs can be partially offset through incentive schemes, such as tax credits. Furthermore, many of the benefits provided by green walls—including aesthetic enhancement, biodiversity support, and improvements in environmental quality and well-being—are difficult to monetize and are therefore often underestimated in conventional economic assessments. Finally, although multi-oriented applications represent the upper range of potential benefits in the simulations, single-orientation applications may be more feasible in practice where façade accessibility, ownership, maintenance or cost constraints limit full façade coverage.

6. Conclusions

This study evaluates the potential of green façades to enhance the climate resilience of the Italian residential buildings for the use category and climatic zones concerned in the analysis, by mitigating indoor overheating and reducing cooling energy needs under both current and future climate scenarios. By applying detailed mathematical modelling of the green façade within EnergyPlus, the research examined various green façade configurations applied to pre- and post-retrofit building conditions across two climate zones of Rome and Turin and three timeframes (2020s, 2050s, and 2090s).

The results indicate that green façades can significantly improve indoor thermal comfort and reduce cooling energy need, especially in pre-retrofit single-unit buildings. Multi-oriented green façades configurations proved most effective for thermal comfort, reducing weighted hours of exceedance by up to 84.6% in Turin and 68.5% in Rome in the 2020s, and lowering cooling needs by up to 59.3% and 51.1%, respectively. Although relative percentage reductions generally decrease as baseline cooling loads and overheating increase, green façades continue to provide relevant absolute benefits under future climates. These results are conditional on maintaining the assumed vegetation coverage and LAI; future studies should quantify irrigation demand, water stress and plant survivability through dynamic, species-specific modelling. However, the contribution of green façades in reducing cooling energy need remains considerable, even in the 2090s, particularly in Rome, where growing summer cooling loads increase the need for passive solutions. Additionally, the lower heating need in Rome makes the energy trade-off associated with green façade shading more favourable than in Turin, where winter heating needs are higher.

Despite the improved performance of post-retrofit single-unit

buildings—benefiting from enhanced insulation, solar control, and ventilative cooling—green façades continue to deliver meaningful cooling reductions. For instance, in the 2050s, multi-oriented green façades reduce cooling needs by 21.2% in Rome and 21.7% in Turin, indicating that their potential contribution is not limited to pre-retrofit buildings. Despite the promising theoretical findings, several technical and economic barriers continue to hinder the widespread adoption of green façades. The most significant constraints include installation and maintenance costs, technical challenges associated with waterproofing and building integration, and the limited willingness of private stakeholders to invest in such systems. Nevertheless, the potential increase in property values, together with the improvement of environmental quality, may contribute to the attractiveness of green façades as effective strategies for enhancing urban sustainability and supporting climate-resilient building design, although the techno-economic aspects were not quantitatively assessed in the present study. To further promote their large-scale implementation, dedicated urban policies and financial incentive mechanisms should support their deployment. In this context, some countries and municipalities have already adopted pioneering initiatives. For example, the Vancouver City Council endorsed, in May 2007, the Passive Design Toolkits, which include green wall implementation in new buildings [107]. Similarly, the municipality of Cologne provides subsidies covering up to 50% of eligible costs, with a maximum annual contribution of € 20,000 (up to 40 €/m^2), to encourage the deployment of green roofs and green walls [108].

The results are valid for the building stock represented by the analysed archetype, and results cannot be transferred to other building typologies, construction periods, urban morphologies and climatic zones. Nevertheless, the proposed methodology can be replicated and adapted to investigate other contexts in future studies. Moreover, future research should also expand the scope to include other types of vertical greenery systems, such as living walls. Additionally, analyses will incorporate the broader urban context, including interactions with the microclimate, urban form, and street canyon geometry, to fully capture the synergistic effects of façade greening at the neighbourhood or city scale. Furthermore, experimental validation of the simulation framework, particularly for the analysed climatic contexts, building archetype and retrofit configurations, post occupancy evaluation, and techno-economic assessment of installation and operational costs are identified as important priorities to further consolidate and extend the findings of the present study.

Overall, this study provides simulation-based evidence that green façades, and multi-oriented configurations in particular, can improve the climate resilience of the analysed residential building archetype in the two climatic contexts considered. Within the adopted modelling assumptions, the simulations indicate that these benefits are consistent for the analysed archetype in both climatic contexts, delivering summer cooling savings and improved indoor comfort that grow under future climate scenarios. The net annual balance between summer savings and winter heating penalties depends on climate and building state, and becomes more favourable as cooling demand grows and in well-insulated post-retrofit buildings, with the strongest overall balance observed in the warmer climatic context analysed. Further generalisation of these findings beyond the analysed archetype and climatic contexts would benefit from case-specific experimental validation, post-occupancy evaluation and techno-economic assessment, which are needed to assess the robustness, real-world performance and practical feasibility of the simulated configurations. Pending such evidence, the results should be regarded as simulation-based evidence supporting further investigation rather than as validated design recommendations or policy prescriptions to inform large-scale renovation strategies or urban greening incentives. They nevertheless provide a basis for future validation and for assessing the potential role of green façades in building renovation and climate adaptation strategies. Where such measures are considered, particular attention should be given to resilient vegetation species, adaptable irrigation systems, and solutions capable of maintaining year-round energy performance while delivering wider urban co-benefits.

CRediT authorship contribution statement

Mamak P. Tootkaboni: Writing – original draft, Visualization, Software, Resources, Methodology, Investigation, Formal analysis, Data curation, Conceptualization. **Ilaria Ballarini:** Writing – review & editing, Validation, Resources, Project administration, Methodology, Investigation, Data curation, Conceptualization. **Vincenzo Corrado:** Writing – review & editing, Validation, Supervision, Project administration, Methodology, Data curation, Conceptualization. **Tiziana Susca:** Writing – review & editing, Writing – original draft, Supervision, Project administration, Methodology, Investigation, Funding acquisition, Conceptualization. **Fabio Zanghirella:** Writing – review & editing, Writing – original draft, Supervision, Project administration, Methodology, Investigation, Funding acquisition, Conceptualization.

Declaration of competing interest

The authors declare the following financial interests/personal relationships which may be considered as potential competing interests: Tiziana Susca and Fabio Zanghirella reports financial support was provided by ENEA National Agency for New Technologies Energy and Economic Sustainable Development. If there are other authors, they declare that they have no known competing financial interests or personal relationships that could have appeared to influence the work reported in this paper.

Acknowledgements

This research was funded by ENEA within the framework of the Electric System Research Programme (Three-Year Implementation Plan 2025–2027), Project 1.5 “High efficiency buildings for the energy transition”, Work Package 4 “Promotion of building energy efficiency through increasing autonomy, flexibility and awareness of energy consumption”, financed by the Italian Ministry for the Environment and Energy Security. CUP: I53C24003330001.

Table A.1
Thermal comfort indicators (Rome – Pre-retrofit).

Climate Scenarios	Strategies	*HE* (h)	*WHE* (h)	*HE* variation vs Baseline (−)	*WHE* variation vs Baseline (−)
2020s	Baseline	1877	3475	–	–
	South-facing green façade	1760	2989	−6.2%	−14.0%
	Multi-oriented green façades	834	1094	−55.6%	−68.5%
2050s	Baseline	1985	4107	–	–
	South-facing green façade	1825	3565	−8.1%	−13.2%
	Multi-oriented green façades	1333	1988	−32.8%	−51.6%
2090s	Baseline	2139	5275	–	–
	South-facing green façade	2057	4804	−3.8%	−8.9%
	Multi-oriented green façades	1559	3184	−27.1%	−39.6%

Table A.2
Thermal comfort indicators (Turin – Pre-retrofit).

(*continued on next page*)

Table A.2 (*continued*)

Climate Scenarios	Strategies	*HE* (h)	*WHE* (h)	*HE* variation vs Baseline (−)	*WHE* variation vs Baseline (−)
Climate Scenarios	Strategies	*HE* (h)	*WHE* (h)	*HE* variation vs Baseline (−)	*WHE* variation vs Baseline (−)
2020s	Baseline	747	1103	–	–
	South-facing green façade	552	769	−26.1%	−30.3%
	Multi-oriented green façades	135	170	−81.9%	−84.6%
2050s	Baseline	1103	1635	–	–
	South-facing green façade	835	1153	−24.3%	−29.5%
	Multi-oriented green façades	280	335	−74.6%	−79.5%
2090s	Baseline	1520	2825	–	–
	South-facing green façade	1360	2360	−10.5%	−16.5%
	Multi-oriented green façades	878	1322	−42.2%	−53.2%

Table A.3
Thermal comfort indicators (Rome – Post-retrofit + ventilative cooling).

Climate Scenarios	Strategies	*HE* (h)	*WHE* (h)	*HE* variation vs Baseline (−)	*WHE* variation vs Baseline (−)
2020s	Baseline	592	774	–	–
	South-facing green façade	551	701	−6.9%	−9.4%
	Multi-oriented green façades	359	416	−39.4%	−46.3%
2050s	Baseline	1162	1638	–	–
	South-facing green façade	1068	1484	−8.1%	−9.4%
	Multi-oriented green façades	807	1052	−30.6%	−35.8%
2090s	Baseline	1310	2906	–	–
	South-facing green façade	1288	2818	−1.7%	−3.0%
	Multi-oriented green façades	1232	2539	−6.0%	−12.6%

Table A.4
Thermal comfort indicators (Turin – Post-retrofit + ventilative cooling).

Climate Scenarios	Strategies	*HE* (h)	*WHE* (h)	*HE* variation vs Baseline (−)	*WHE* variation vs Baseline (−)
2020s	Baseline	125	135	–	–
	South-facing green façade	102	109	−18.4%	−19.3%
	Multi-oriented green façades	101	107	−19.2%	−20.7%
2050s	Baseline	366	416	–	–
	South-facing green façade	221	240	−39.6%	−42.3%
	Multi-oriented green façades	175	188	−52.2%	−54.8%
2090s	Baseline	912	1256	–	–
	South-facing green façade	858	1161	−5.9%	−7.6%
	Multi-oriented green façades	781	1009	−14.4%	−19.7%

Table A.5
Energy performance indicators (Rome – Pre-retrofit).

Climate Scenarios	Strategies	$EP_{C,nd}$ (kWh·m^{-2})	$EP_{H,nd}$ (kWh·m^{-2})	$EP_{C,nd}$ + $EP_{H,nd}$ (kWh·m^{-2})	$EP_{C,nd}$ variation vs Baseline (−)	$EP_{H,nd}$ variation vs Baseline (−)	$EP_{C,nd}$ + $EP_{H,nd}$ variation vs Baseline (−)
2020s	Baseline	32.1	57.0	89.1	–	–	–
	South-facing green façade	27.2	64.5	91.7	−15.3%	13.2%	2.9%
	Multi-oriented green façades	15.7	74.3	90.0	−51.1%	30.4%	1.0%
2050s	Baseline	42.8	35.2	78.0	–	–	–
	South-facing green façade	36.7	41.2	77.9	−14.3%	17.0%	−0.1%
	Multi-oriented green façades	22.8	48.3	71.1	−46.7%	37.2%	−8.8%
2090s	Baseline	65.0	14.9	79.9	–	–	–
	South-facing green façade	57.8	19.0	76.8	−11.1%	27.5%	−3.9%
	Multi-oriented green façades	40.7	23.6	64.3	−37.4%	58.4%	−19.5%

Table A.6
Energy performance indicators (Turin – Pre-retrofit).

Climate Scenarios	Strategies	$EP_{C,nd}$ (kWh·m^{-2})	$EP_{H,nd}$ (kWh·m^{-2})	$EP_{C,nd}$ + $EP_{H,nd}$ (kWh·m^{-2})	$EP_{C,nd}$ variation vs Baseline (−)	$EP_{H,nd}$ variation vs Baseline (−)	$EP_{C,nd}$ + $EP_{H,nd}$ variation vs Baseline (−)
2020s	Baseline	13.5	112.6	126.1	–	–	–
	South-facing green façade	10.4	121.3	131.7	−23.0%	7.7%	4.4%
	Multi-oriented green façades	5.5	128.5	134.0	−59.3%	14.2%	6.3%
2050s	Baseline	18.8	100.0	118.8	–	–	–
	South-facing green façade	15.2	108.1	123.3	−19.1%	8.1%	3.8%
	Multi-oriented green façades	9.3	114.9	124.2	−50.5%	14.9%	4.5%
2090s	Baseline	36.1	72.8	108.9	–	–	–
	South-facing green façade	30.3	79.3	109.6	−16.0%	8.9%	0.6%
	Multi-oriented green façades	21.1	83.9	105	−41.5%	15.1%	−3.6%

Table A.7
Energy performance indicators (Rome – Post-retrofit + ventilative cooling).

Climate Scenarios	Strategies	$EP_{C,nd}$ (kWh·m^{-2})	$EP_{H,nd}$ (kWh·m^{-2})	$EP_{C,nd}$ + $EP_{H,nd}$ (kWh·m^{-2})	$EP_{C,nd}$ variation vs Baseline (−)	$EP_{H,nd}$ variation vs Baseline (−)	$EP_{C,nd}$ + $EP_{H,nd}$ variation vs Baseline (−)
2020s	Baseline	19.0	8.1	27.1	–	–	–
	South-facing green façade	17.9	9.1	27.0	−5.8%	12.3%	−0.4%
	Multi-oriented	14.7	10.5	25.2	−22.6%	29.6%	−7.0%

(*continued on next page*)

Table A.7 (*continued*)

Climate Scenarios	Strategies	$EP_{C,nd}$ (kWh·m^{-2})	$EP_{H,nd}$ (kWh·m^{-2})	$EP_{C,nd}$ + $EP_{H,nd}$ (kWh·m^{-2})	$EP_{C,nd}$ variation vs Baseline (–)	$EP_{H,nd}$ variation vs Baseline (–)	$EP_{C,nd}$ + $EP_{H,nd}$ variation vs Baseline (–)
	green façades						
2050s	Baseline	26.0	2.4	28.4	–	–	–
	South-facing green façade	24.6	2.9	27.5	−5.4%	20.8%	−3.2%
	Multi-oriented green façades	20.5	3.6	24.1	−21.2%	50.0%	−15.1%
2090s	Baseline	37.5	0.0	37.5	–	–	–
	South-facing green façade	35.9	0.1	36.0	−4.3%	0.0%	−4.0%
	Multi-oriented green façades	31.3	0.1	31.4	−16.5%	0.0%	−16.3%

Table A.8
Energy performance indicators (Turin – Post-retrofit + ventilative cooling).

Climate Scenarios	Strategies	$EP_{C,nd}$ (kWh·m^{-2})	$EP_{H,nd}$ (kWh·m^{-2})	$EP_{C,nd}$ + $EP_{H,nd}$ (kWh·m^{-2})	$EP_{C,nd}$ variation vs Baseline (–)	$EP_{H,nd}$ variation vs Baseline (–)	$EP_{C,nd}$ + $EP_{H,nd}$ variation vs Baseline (–)
2020s	Baseline	8.5	19.5	28	–	–	–
	South-facing green façade	7.8	20.4	28.2	−8.2%	4.6%	0.7%
	Multi-oriented green façades	6.4	21.2	27.6	−24.7%	8.7%	−1.4%
2050s	Baseline	12.0	16.4	28.4	–	–	–
	South-facing green façade	11.1	17.5	28.6	−7.5%	6.7%	0.7%
	Multi-oriented green façades	9.4	18.2	27.6	−21.7%	11.0%	−2.8%
2090s	Baseline	21.8	10.1	31.9	–	–	–
	South-facing green façade	20.4	10.9	31.3	−6.4%	7.9%	−1.9%
	Multi-oriented green façades	18.0	11.4	29.4	−17.4%	12.9%	−7.8%

References

[1] Directorate-General for Energy (European Commission), EU energy in figures: statistical pocketbook 2024, Publications Office of the European Union, 2024. https://data.europa.eu/doi/10.2833/802460. accessed June 30, 2025.

[2] Z.J. Zhai, J.M. Helman, Implications of climate changes to building energy and design, Sustain. Cities Soc. 44 (2019) 511–519, https://doi.org/10.1016/j.scs.2018.10.043.

[3] U.Y. Ayikoe Tettey, L. Gustavsson, Energy savings and overheating risk of deep energy renovation of a multi-storey residential building in a cold climate under climate change, Energy 202 (2020) 117578, https://doi.org/10.1016/j.energy.2020.117578.

[4] E. Rodrigues, M.S. Fernandes, Overheating risk in Mediterranean residential buildings: comparison of current and future climate scenarios, Appl. Energy 259 (2020) 114110, https://doi.org/10.1016/j.apenergy.2019.114110.

[5] World Bank, Urban population (% of total population). https://data.worldbank.org/indicator/SP.URB.TOTL.IN.ZS, 2024 (accessed June 11, 2025).

[6] K.R. Gurney, Ş. Kılkış, K.C. Seto, S. Lwasa, D. Moran, K. Riahi, M. Keller, P. Rayner, M. Luqman, Greenhouse gas emissions from global cities under SSP/RCP scenarios, 1990 to 2100, Glob. Environ. Chang. 73 (2022) 102478, https://doi.org/10.1016/j.gloenvcha.2022.102478.

[7] M.P. McCarthy, M.J. Best, R.A. Betts, Climate change in cities due to global warming and urban effects, Geophys. Res. Lett. 37 (2010), https://doi.org/10.1029/2010GL042845.

[8] D. Li, W. Liao, A.J. Rigden, X. Liu, D. Wang, S. Malyshev, E. Shevliakova, Urban heat island: aerodynamics or imperviousness? Sci. Adv. 5 (2019) https://doi.org/10.1126/sciadv.aau4299.

[9] S.E. Cleland, W. Steinhardt, L.M. Neas, J. Jason West, A.G. Rappold, Urban heat island impacts on heat-related cardiovascular morbidity: a time series analysis of older adults in US metropolitan areas, Environ. Int. 178 (2023) 108005, https://doi.org/10.1016/j.envint.2023.108005.

[10] W.T.K. Huang, P. Masselot, E. Bou-Zeid, S. Fatichi, A. Paschalis, T. Sun, A. Gasparrini, G. Manoli, Economic valuation of temperature-related mortality attributed to urban heat islands in European cities, Nat. Commun. 14 (2023) 7438, https://doi.org/10.1038/s41467-023-43135-z.

[11] X. Li, Y. Zhou, S. Yu, G. Jia, H. Li, W. Li, Urban heat island impacts on building energy consumption: a review of approaches and findings, Energy 174 (2019) 407–419, https://doi.org/10.1016/j.energy.2019.02.183.

[12] C. Chessa, T. Susca, Development of an LCA characterization factor to account UHI local effect on terrestrial ecosystems damage category: evaluation of European Bombus and Onthophagus genera heat-stress mortality, Sci. Total Environ. 897 (2023) 165183, https://doi.org/10.1016/j.scitotenv.2023.165183.

[13] R. Cichowicz, A.D. Bochenek, Assessing the effects of urban heat islands and air pollution on human quality of life, Anthropocene 46 (2024) 100433, https://doi.org/10.1016/j.ancene.2024.100433.

[14] M. Santamouris, C. Cartalis, A. Synnefa, D. Kolokotsa, On the impact of urban heat island and global warming on the power demand and electricity consumption of buildings—a review, Energ. Buildings 98 (2015) 119–124, https://doi.org/10.1016/j.enbuild.2014.09.052.

[15] M. Košir, L. Pajek, N. Iglič, R. Kunič, A theoretical study on a coupled effect of building envelope solar properties and thermal transmittance on the thermal response of an office cell, Sol. Energy 174 (2018) 669–682, https://doi.org/10.1016/j.solener.2018.09.042.

[16] G. Tomrukcu, T. Ashrafian, Climate-resilient building energy efficiency retrofit: evaluating climate change impacts on residential buildings, Energ. Buildings 316 (2024) 114315, https://doi.org/10.1016/j.enbuild.2024.114315.

[17] M.P. Tootkaboni, I. Ballarini, V. Corrado, Towards climate resilient and energy-efficient buildings: a sensitivity analysis on building components and cooling strategies, Build. Environ. 270 (2025) 112473, https://doi.org/10.1016/j.buildenv.2024.112473.

[18] G. Brunetta, D. Mohabat Doost, E. Berisha, G. Garnero, F. Pellerey, C. Tedesco, B. Pincegher, Mapping territorial vulnerability for resilience planning. The R3C-GeoResilience tool applied to the Union of Bassa Romagna (Italy), Urban Sci. 9 (2025) 400, https://doi.org/10.3390/urbansci9100400.

[19] D. Mohabat Doost, G. Brunetta, Just territorial resilience: disentangling EU policy narratives between geopolitical stability and spatial justice, 2026, https://doi.org/10.5281/ZENODO.20340705.

[20] P. Holzer, P. Stern, P. Czarnecki, D.-I. Bogatu, E. Bozonnet, H. Breesch, V. Corrado, G. Gediz Ilis, P. Jaboyedoff, O.B. Kazanci, T. Keller, B. Kling, A. Krelling, S.H. Lee, R. Levinson, M.P. Tootkaboni, T. Psomas, D. Qi, C. Rzihacek, M. Wolf, M. Zinzi, International energy agency - resilient cooling of buildings - technology profiles report (annex 80), Institute of Building Research & Innovation, 2024, https://doi.org/10.52776/HFTR4661.

[21] C. Zhang, O.B. Kazanci, R. Levinson, P. Heiselberg, B.W. Olesen, G. Chiesa, B. Sodagar, Z. Ai, S. Selkowitz, M. Zinzi, A. Mahdavi, H. Teufl, M. Kolokotroni, A. Salvati, E. Bozonnet, F. Chtioui, P. Salagnac, R. Rahif, S. Attia, V. Lemort, E. Elnagar, H. Breesch, A. Sengupta, L.L. Wang, D. Qi, P. Stern, N. Yoon, D.-I. Bogatu, R.F. Rupp, T. Arghand, S. Javed, J. Akander, A. Hayati, M. Cehlin, S. Sayadi, S. Forghani, H. Zhang, E. Arens, G. Zhang, Resilient cooling strategies – a critical review and qualitative assessment, Energ. Buildings 251 (2021) 111312, https://doi.org/10.1016/j.enbuild.2021.111312.

[22] T. Psomas, V. Corrado (Eds.), Resilient Cooling Design Guidelines, REHVA – Federation of European Heating, Ventilation and Air Conditioning Associations, Brussels, Belgium, 2024. https://www.rehva.eu/eshop/detail/resilient-cooling-design-guidelines.

[23] G.L. Feyisa, K. Dons, H. Meilby, Efficiency of parks in mitigating urban heat island effect: an example from Addis Ababa, Landsc. Urban Plan. 123 (2014) 87–95, https://doi.org/10.1016/j.landurbplan.2013.12.008.

[24] C.P. Skelhorn, G. Levermore, S.J. Lindley, Impacts on cooling energy consumption due to the UHI and vegetation changes in Manchester, UK, Energ. Buildings 122 (2016) 150–159, https://doi.org/10.1016/j.enbuild.2016.01.035.

[25] T. Susca, Nature-based solutions applied to the built environment to alleviate climate change: benefits, co-benefits, and trade-offs in a geographical multi-scale perspective, in: Handb. Clim. Change Mitig. Adapt., Springer, Cham, 2022, pp. 2117–2167, https://doi.org/10.1007/978-3-030-72579-2_123.

[26] J. Iaria, T. Susca, Analytic hierarchy processes (AHP) evaluation of green roof- and green wall- based UHI mitigation strategies via ENVI-met simulations, Urban Clim. 46 (2022) 101293, https://doi.org/10.1016/j.uclim.2022.101293.

[27] T. Susca, J. Iaria, F. Zanghirella, Development of predictive indices for evaluating the UHI adaptation potential of green roof- and wall-based scenarios in the Mediterranean climate, Sci. Rep. 14 (2024) 21675, https://doi.org/10.1038/s41598-024-67567-9.

[28] M. Köhler, Green facades—a view back and some visions, Urban Ecosyst. 11 (2008) 423–436, https://doi.org/10.1007/s11252-008-0063-x.

[29] T. Susca, Nature-Based Solutions Applied to the Built Environment to Alleviate Climate Change: A Geographical Multi-Scale Perspective, in: Handb. Clim. Change Mitig. Adapt., Springer, New York, NY, 2024, pp. 1–42, https://doi.org/10.1007/978-1-4614-6431-0_123-3.

[30] T.E. Morakinyo, A. Lai, K.K.-L. Lau, E. Ng, Thermal benefits of vertical greening in a high-density city: case study of Hong Kong, Urban For. Urban Green. 37 (2019) 42–55, https://doi.org/10.1016/j.ufug.2017.11.010.
[31] G. Pérez, J. Coma, S. Sol, L.F. Cabeza, Green facade for energy savings in buildings: the influence of leaf area index and facade orientation on the shadow effect, Appl. Energy 187 (2017) 424–437, https://doi.org/10.1016/j.apenergy.2016.11.055.
[32] K. Perini, M. Ottelé, A. Fraaij, E. Haas, R. Raiteri, Vertical greening systems and the effect on air flow and temperature on the building envelope, Build. Environ. 46 (2011) 2287–2294, https://doi.org/10.1016/j.buildenv.2011.05.009.
[33] T. Susca, F. Zanghirella, V. Del Fatto, Building integrated vegetation effect on micro-climate conditions for urban heat island adaptation. Lesson learned from Turin and Rome case studies, Energ. Buildings 295 (2023) 113233, https://doi.org/10.1016/j.enbuild.2023.113233.
[34] T. Susca, F. Zanghirella, L. Colasuonno, V. Del Fatto, Effect of green wall installation on urban heat island and building energy use: a climate-informed systematic literature review, Renew. Sust. Energ. Rev. 159 (2022) 112100, https://doi.org/10.1016/j.rser.2022.112100.
[35] Z. Azkorra, G. Pérez, J. Coma, L.F. Cabeza, S. Bures, J.E. Álvaro, A. Erkoreka, M. Urrestarazu, Evaluation of green walls as a passive acoustic insulation system for buildings, Appl. Acoust. 89 (2015) 46–56, https://doi.org/10.1016/j.apacoust.2014.09.010.
[36] J. Lu, F. Kong, H. Yin, J. Kang, H. Liu, Z. Li, H. Huang, K. Zhou, S. Yang, Extensive green roofs for noise abatement: combined acoustic effects of substrate and vegetation in a 3D environment, Build. Environ. 270 (2025) 112545, https://doi.org/10.1016/j.buildenv.2025.112545.
[37] M. Tomson, P. Kumar, Y. Barwise, P. Perez, H. Forehead, K. French, L. Morawska, J.F. Watts, Green infrastructure for air quality improvement in street canyons, Environ. Int. 146 (2021) 106288, https://doi.org/10.1016/j.envint.2020.106288.
[38] M.R. Seyedabadi, U. Eicker, S. Karimi, Plant selection for green roofs and their impact on carbon sequestration and the building carbon footprint, Environ. Chall. 4 (2021) 100119, https://doi.org/10.1016/j.envc.2021.100119.
[39] X. Qian, X. Zhang, A.U. Weerasuriya, J. Zhai, Designing green walls to mitigate fine particulate pollution in an idealized urban environment, Sustain. Cities Soc. 113 (2024) 105640, https://doi.org/10.1016/j.scs.2024.105640.
[40] J. Yan, L. Zhao, Z. Nie, S. Chen, Synergistic carbon sequestration and emission reduction of green facades: climate-specific analysis for office buildings, Energ. Buildings 347 (2025) 116336, https://doi.org/10.1016/j.enbuild.2025.116336.
[41] J.C. Berndtsson, L. Bengtsson, K. Jinno, Runoff water quality from intensive and extensive vegetated roofs, Ecol. Eng. 35 (2009) 369–380, https://doi.org/10.1016/j.ecoleng.2008.09.020.
[42] W. Liu, W. Wei, W. Chen, R.C. Deo, J. Si, H. Xi, B. Li, Q. Feng, The impacts of substrate and vegetation on stormwater runoff quality from extensive green roofs, J. Hydrol. 576 (2019) 575–582, https://doi.org/10.1016/j.jhydrol.2019.06.061.
[43] M. Moravej, C. Swinbourne, R. Hall, S. Kenway, Vertical green systems (VGSs) and on-site storage for stormwater management, Water Res. 281 (2025) 123560, https://doi.org/10.1016/j.watres.2025.123560.
[44] A. Galvão, M. Rodrigues, J. Mata, C.M. Silva, Green walls for greywater treatment: a comprehensive review of operational parameters and climate influence on treatment performance, Water Res. 272 (2025) 122948, https://doi.org/10.1016/j.watres.2024.122948.
[45] P. Ndayambaje, J.S. MacIvor, M.W. Cadotte, Plant diversity on green roofs: a review of the ecological benefits, challenges, and best management practices, Nat.-Based Solut. 6 (2024) 100162, https://doi.org/10.1016/j.nbsj.2024.100162.
[46] R. Collins, M. Schaafsma, M.D. Hudson, The value of green walls to urban biodiversity, Land Use Policy 64 (2017) 114–123, https://doi.org/10.1016/j.landusepol.2017.02.025.
[47] K.J.H. Williams, K.E. Lee, L. Sargent, K.A. Johnson, J. Rayner, C. Farrell, R. E. Miller, N.S.G. Williams, Appraising the psychological benefits of green roofs for city residents and workers, Urban For. Urban Green. 44 (2019) 126399, https://doi.org/10.1016/j.ufug.2019.126399.
[48] M. Goel, B. Jha, S. Khan, Living walls enhancing the urban realm: a review, Environ. Sci. Pollut. Res. Int. 29 (2022) 38715–38734, https://doi.org/10.1007/s11356-022-19501-7.
[49] Y. Liu, H. Wang, W. Li, Y. Li, Effects of green-wall layouts on psychological and physiological responses in office environments: a virtual-environment study, Front. Psychol. 16 (2025) 1711317, https://doi.org/10.3389/fpsyg.2025.1711317.
[50] W. Knifka, R. Karutz, H. Zozmann, Barriers and solutions to green facade implementation—a review of literature and a case study of Leipzig, Germany, Buildings 13 (2023) 1621, https://doi.org/10.3390/buildings13071621.
[51] B. Riley, The state of the art of living walls: lessons learned, Build. Environ. 114 (2017) 219–232, https://doi.org/10.1016/j.buildenv.2016.12.016.
[52] F. Ascione, R.F. De Masi, M. Mastellone, S. Ruggiero, G.P. Vanoli, Green walls, a critical review: knowledge gaps, design parameters, thermal performances and multi-criteria design approaches, Energies 13 (2020) 2296, https://doi.org/10.3390/en13092296.
[53] E. Oberndorfer, J. Lundholm, B. Bass, R.R. Coffman, H. Doshi, N. Dunnett, S. Gaffin, M. Köhler, K.K.Y. Liu, B. Rowe, Green roofs as urban ecosystems: ecological structures, functions, and services, BioScience 57 (2007) 823–833, https://doi.org/10.1641/B571005.
[54] E. Cristiano, D. Pumo, F. Boano, M. Ippolito, F. Viola, Citizens' perception and willingness to pay for green roofs and nature-based solutions in three Italian metropolitan cities, Urban For. Urban Green. 112 (2025) 128928, https://doi.org/10.1016/j.ufug.2025.128928.
[55] S.W. Tsang, C.Y. Jim, Game-theory approach for resident coalitions to allocate green-roof benefits, Environ. Plann. A: Econ. Space 43 (2011) 363–377, https://doi.org/10.1068/a43230.
[56] S. Cascone, F. Catania, A. Gagliano, G. Sciuto, A comprehensive study on green roof performance for retrofitting existing buildings, Build. Environ. 136 (2018) 227–239, https://doi.org/10.1016/j.buildenv.2018.03.052.
[57] M. Molari, L. Dominici, M. Manso, C.M. Silva, E. Comino, A socio-ecological approach to investigate the perception of green walls in cities: a comparative analysis of case studies in Turin and Lisbon, Nat.-Based Solut. 6 (2024) 100175, https://doi.org/10.1016/j.nbsj.2024.100175.
[58] S. Chen, F. Olivieri, L. Peng, J. Li, Benefits and monetary values of vertical greening systems: a semi-systematic review, Build. Environ. 284 (2025) 113463, https://doi.org/10.1016/j.buildenv.2025.113463.
[59] F. Bianchini, K. Hewage, Probabilistic social cost-benefit analysis for green roofs: a lifecycle approach, Build. Environ. 58 (2012) 152–162, https://doi.org/10.1016/j.buildenv.2012.07.005.
[60] K. Ichihara, J.P. Cohen, New York City property values: what is the impact of green roofs on rental pricing? Lett. Spat. Resour. Sci. 4 (2011) 21–30, https://doi.org/10.1007/s12076-010-0046-4.
[61] A. Dehghan Lotfabad, S.M. Hosseini, P. Dabove, M. Heiranipour, F. Sommese, Impacts of vertical greenery on outdoor thermal comfort and carbon emission reduction at the urban scale in Turin, Italy, Buildings 15 (2025) 450, https://doi.org/10.3390/buildings15030450.
[62] L.W. Chew, X.-X. Li, M.Y.L. Chew, Climate change projection and its impacts on building façades in Singapore, Sustainability 15 (2023), https://doi.org/10.3390/su15043156.
[63] I. Andric, A. Kamal, S.G. Al-Ghamdi, Efficiency of green roofs and green walls as climate change mitigation measures in extremely hot and dry climate: case study of Qatar, Energy Rep. 6 (2020) 2476–2489, https://doi.org/10.1016/j.egyr.2020.09.006.
[64] M. Fahmy, H. El-Hady, M. Mahdy, M.F. Abdelalim, On the green adaptation of urban developments in Egypt; predicting community future energy efficiency using coupled outdoor-indoor simulations, Energ. Buildings 153 (2017) 241–261, https://doi.org/10.1016/j.enbuild.2017.08.008.
[65] M. Fahmy, M. Mahdy, S. Mahmoud, M. Abdelalim, S. Ezzeldin, S. Attia, Influence of urban canopy green coverage and future climate change scenarios on energy consumption of new sub-urban residential developments using coupled simulation techniques: a case study in Alexandria, Egypt, Energy Rep. 6 (2020) 638–645, https://doi.org/10.1016/j.egyr.2019.09.042.
[66] V. Nesci, I. Ballarini, P. Rando Mazzarino, V. Corrado, Living walls and green façades: an implementation code for energy simulation, Buildings 14 (2024) 2040, https://doi.org/10.3390/buildings14072040.
[67] E. Cuce, Thermal regulation impact of green walls: an experimental and numerical investigation, Appl. Energy 194 (2017) 247–254, https://doi.org/10.1016/j.apenergy.2016.09.079.
[68] K. Karimi, M. Farrokhzad, G. Roshan, M. Aghdasi, Evaluation of effects of a green wall as a sustainable approach on reducing energy use in temperate and humid areas, Energ. Buildings 262 (2022) 112014, https://doi.org/10.1016/j.enbuild.2022.112014.
[69] M. Manso, J. Castro-Gomes, Green wall systems: a review of their characteristics, Renew. Sust. Energ. Rev. 41 (2015) 863–871, https://doi.org/10.1016/j.rser.2014.07.203.
[70] K. Perini, P. Rosasco, Cost–benefit analysis for green façades and living wall systems, Build. Environ. 70 (2013) 110–121, https://doi.org/10.1016/j.buildenv.2013.08.012.
[71] P. Rosasco, Economic Benefits and Costs of Vertical Greening Systems, in: Nat. Based Strateg. Urban Build. Sustain., Elsevier, 2018, pp. 291–306, https://doi.org/10.1016/B978-0-12-812150-4.00027-6.
[72] L. Dominici, E. Comino, F. Torpy, P. Irga, Vertical greening systems: a critical comparison of do-it-yourself designs, Plants 11 (2022) 3230, https://doi.org/10.3390/plants11233230.
[73] M. Manso, I. Teotónio, C.M. Silva, C.O. Cruz, Green roof and green wall benefits and costs: a review of the quantitative evidence, Renew. Sust. Energ. Rev. 135 (2021) 110111, https://doi.org/10.1016/j.rser.2020.110111.
[74] T.D. De Oliveira Santos, F.A.L. Pacheco, L.F.S. Fernandes, A systematic analysis on the efficiency and sustainability of green facades and roofs, Sci. Total Environ. 932 (2024) 173107, https://doi.org/10.1016/j.scitotenv.2024.173107.
[75] M. Ottelé, K. Perini, A.L.A. Fraaij, E.M. Haas, R. Raiteri, Comparative life cycle analysis for green façades and living wall systems, Energ. Buildings 43 (2011) 3419–3429, https://doi.org/10.1016/j.enbuild.2011.09.010.
[76] R. Bakhshoodeh, C. Ocampo, C. Oldham, Exploring the evapotranspirative cooling effect of a green façade, Sustain. Cities Soc. 81 (2022) 103822, https://doi.org/10.1016/j.scs.2022.103822.
[77] Y. Zhang, L. Zhang, Q. Meng, Dynamic heat transfer model of vertical green façades and its co-simulation with a building energy modelling program in hot-summer/warm-winter zones, J. Build. Eng. 58 (2022) 105008, https://doi.org/10.1016/j.jobe.2022.105008.
[78] C. Zhao, L. Zhang, Y. Yang, Y. Zhang, M. Liu, J. Yan, L. Zhao, Long-wave infrared radiation properties of vertical green façades in subtropical regions, Build. Environ. 223 (2022) 109518, https://doi.org/10.1016/j.buildenv.2022.109518.
[79] P. Holzer, E. Arens, S. Attia, V. Corrado, R. Gupta, M. Hamdy, S. Homaei, A. Laouadi, R. Levinson, S. Selkowitz, A. Sengupta, B. Sodagar, M. Zinzi, L. Wang, G. Abhishek, International energy agency resilient cooling of buildings – key performance indicators report (Annex 80), 2024, https://doi.org/10.52776/RHET5776.

[80] International Organization for Standardization, ISO 17772: Energy performance of buildings – Indoor environmental quality – Part 1 : Indoor environmental input parameters for the design and assessment of energy performance of buildings., 2017.
[81] European Committee for Standardization (CEN), EN ISO 7730, Ergonomics of the Thermal Environment—Analytical Determination and Interpretation of Thermal Comfort Using Calculation of the PMV and PPD Indices and Local Thermal Comfort Criteria, 2005.
[82] International Organization for Standardization, ISO 52000-1:2017.Energy performance of buildings -Overarching EPB assessment -Part 1: General framework and procedures. https://www.iso.org/standard/65601.html, 2017.
[83] International Organization for Standardization, ISO 52016-1: Energy performance of buildings – Energy needs for heating and cooling, internal temperatures, and sensible and latent heat loads – Part 1: Calculation procedures, 2017.
[84] V. Corrado, I. Ballarini, S.P. Corgnati, Typology Approach for Building Stock Energy Assessment. D6.2 National scientific report on the TABULA activities in Italy, Politecnico di Torino – Dipartimento Energia, 2012.
[85] I. Ballarini, V. Corrado, A new methodology for assessing the energy consumption of building stocks, Energies 10 (2017) 1102, https://doi.org/10.3390/en10081102.
[86] V. Corrado, I. Ballarini, Refurbishment trends of the residential building stock: analysis of a regional pilot case in Italy, Energ. Buildings 132 (2016) 91–106, https://doi.org/10.1016/j.enbuild.2016.06.022.
[87] I. Ballarini, S. Pichierri, V. Corrado, Tracking the energy refurbishment processes in residential building stocks. The pilot case of Piedmont Region, Energy Procedia 78 (2015) 1051–1056, https://doi.org/10.1016/j.egypro.2015.11.069.
[88] M.P. Tootkaboni, I. Ballarini, V. Corrado, Analysing the future energy performance of residential buildings in the most populated Italian climatic zone: a study of climate change impacts, Energy Rep. 7 (2021) 8548–8560, https://doi.org/10.1016/j.egyr.2021.04.012.
[89] Istituto Nazionale di Statistica (ISTAT), 15° Censimento della popolazione e delle abitazioni 2011. https://www.istat.it/statistiche-per-temi/censimenti/censimenti-storici/popolazione-e-abitazioni/popolazione-2011/, 2011 (accessed September 27, 2026).
[90] Italian Republic, Interministerial decree of June 26th, 2015—calculation methodologies of the building Energy Performance and Minimum Energy Performance Requirements, 2015.
[91] The Italian national organisation for standardisation (UNI), UNI/TS 11300–1: 2014–Energy performance of buildings Part 1: Evaluation of energy need for space heating and cooling, 2014.
[92] A. Belleri, G. Chiesa, Ventilative cooling potential tool. user guide. IEA – EBC programme – Annex 62 ventilative cooling, IEA – EBC Programme, Annex 62 Ventilative Cooling, 2016.
[93] A. O'Donnavan, A. Belleri, F. Flourentzou, G.-Q. Zhang, G.C. da Graca, H. Breesch, M. Justo-Alonso, M. Kolokotroni, M.Z. Pomianowski, P. O'Sullivan, P. K. Heiselberg, P. Holzer, T.Ch. Psomas, Ventilative Cooling Design Guide: Energy in Buildings and Communities Programme., Department of Civil Engineering, Aalborg University, Aalborg, 2018.
[94] Comitato Termotecnico Italiano, Technical Commission 241, in: Italian National Annex of the EN 16798–1 technical standard 181, 2020.
[95] M. Manso, J. Castro-Gomes, Green wall systems: a review of their characteristics, Renew. Sust. Energ. Rev. 41 (2015) 863–871, https://doi.org/10.1016/j.rser.2014.07.203.
[96] M. Radić, M. Brković Dodig, T. Auer, Green facades and living walls—a review establishing the classification of construction types and mapping the benefits, Sustainability 11 (2019) 4579, https://doi.org/10.3390/su11174579.
[97] T. Safikhani, A.M. Abdullah, D.R. Ossen, M. Baharvand, A review of energy characteristic of vertical greenery systems, Renew. Sust. Energ. Rev. 40 (2014) 450–462, https://doi.org/10.1016/j.rser.2014.07.166.
[98] International Organization for Standardization, ISO 9050:2003: Glass in building - Determination of light transmittance, solar direct transmittance, total solar energy transmittance, ultraviolet transmittance and related glazing factors, 2003.
[99] American National Standards Institute (ASHRAE), Climatic Data for Building Design Standards, 2021.
[100] F. Rubel, M. Kottek, Observed and projected climate shifts 1901-2100 depicted by world maps of the Köppen-Geiger climate classification, Meteorol. Z. 19 (2010) 135–141, https://doi.org/10.1127/0941-2948/2010/0430.
[101] A. Machard, A. Salvati, M.P. Tootkaboni, A. Gaur, J. Zou, L.L. Wang, F. Baba, H. Ge, F. Bre, E. Bozonnet, V. Corrado, X. Luo, R. Levinson, S.H. Lee, T. Hong, M. Salles Olinger, R.M. e S. Machado, E.L.A. da Guarda, R.K. Veiga, R. Lamberts, A. Afshari, D. Ramon, H. Ngoc Dung Ngo, A. Sengupta, H. Breesch, N. Heijmans, J. Deltour, X. Kuborn, S. Sayadi, B. Qian, C. Zhang, R. Rahif, S. Attia, P. Stern, P. Holzer, Typical and extreme weather datasets for studying the resilience of buildings to climate change and heatwaves, Sci. Data 11 (2024) 531, https://doi.org/10.1038/s41597-024-03319-8.
[102] E. Coppola, R. Nogherotto, J.M. Ciarlo', F. Giorgi, E. Van Meijgaard, N. Kadygrov, C. Iles, L. Corre, M. Sandstad, S. Somot, P. Nabat, R. Vautard, G. Levavasseur, C. Schwingshackl, J. Sillmann, E. Kjellström, G. Nikulin, E. Aalbers, G. Lenderink, O.B. Christensen, F. Boberg, S.L. Sørland, M. Demory, K. Bülow, C. Teichmann, K. Warrach-Sagi, V. Wulfmeyer, Assessment of the European climate projections as simulated by the large EURO-CORDEX regional and global climate model ensemble, J. Geophys. Res. Atmos. 126 (2021) e2019JD032356, https://doi.org/10.1029/2019JD032356.
[103] R. Bonanno, E. Collino, Assessing the impact of climate change on solar energy production in Italy, Reg. Environ. Chang. 25 (2025) 78, https://doi.org/10.1007/s10113-025-02417-6.
[104] K. Perini, P. Rosasco, Cost–benefit analysis for green façades and living wall systems, Build. Environ. 70 (2013) 110–121, https://doi.org/10.1016/j.buildenv.2013.08.012.
[105] T. Engel, N. Werther, Fire safety for green façades: part 1: basics, state-of-the-art research and experimental investigation of plant flammability, Fire. Technol 60 (2024) 2177–2230, https://doi.org/10.1007/s10694-024-01566-0.
[106] T. Engel, J. Kahler, Fire safety for green façades: part 2: full-scale façade fire tests and means for fire-safe green façade design with climbing plants on trellises, Fire. Technol 62 (2026) 51, https://doi.org/10.1007/s10694-025-01826-7.
[107] City of Vancouver, Planning Department, Passive Design: Demountable Green Walls, City of Vancouver, 2011. https://guidelines.vancouver.ca/bulletins/bulletin-sustainability-passive-design-demountable-green-walls.pdf (accessed May 20, 2026).
[108] Stadt Köln, Funding Programme for Green Infrastructure, Stadt Köln City Cologne, 2018. https://www.stadt-koeln.de/artikel/67044/index.html (accessed May 20, 2026).